

Frederike Klimm  
frederike.klimm@neptun.uni-freiburg.de

# Resonant Ultrasound Spectroscopy

**Analysis of thickness resonances for the characterization of layered materials**

Internship Project Report

01.04.2016 - 15.07.2016

Supervisor  
Prof. Marc Desmulliez

Second supervisor  
Dr. Anne Bernassau

Heriot-Watt-University, Edinburgh

# Contents

<b>1. Introduction</b>	<b>3</b>
<b>2. Literature and theory</b>	<b>5</b>
2.1. Basis . . . . .	5
2.1.1. Ultrasound . . . . .	5
Ultrasonic wave . . . . .	5
Ultrasonic properties . . . . .	6
Interaction of waves . . . . .	9
2.1.2. Ultrasonic transducers . . . . .	11
2.1.3. Signal processing . . . . .	13
2.2. Ultrasonic measurement techniques . . . . .	14
2.2.1. (Conventional) ultrasound techniques . . . . .	14
2.2.2. Resonant Ultrasound Spectroscopy (RUS) . . . . .	16
2.2.3. Broadband ultrasonic spectroscopy . . . . .	16
2.2.4. Air-coupled ultrasonic spectroscopy ("Non-Contact RUS") . . . . .	17
2.3. Ultrasonic Spectroscopy . . . . .	18
2.3.1. Overview . . . . .	18
2.3.2. Modeling the transmission coefficient (one-layer model) . . . . .	22
2.3.3. Limits of the one-layer approach and models for more layers . . . . .	24
Two-layer model . . . . .	26
Three-layer model . . . . .	27
Four-layer model . . . . .	27
2.4. Biological relevance . . . . .	29
<b>3. Experimental work</b>	<b>33</b>
3.1. Methods . . . . .	33
3.1.1. Experimental setup . . . . .	33
3.1.2. Data analysis . . . . .	34
3.2. Results and discussion . . . . .	36
3.2.1. Characterization of setup . . . . .	36
Distance between transducer and receiver . . . . .	36
Introduction of a sample . . . . .	37
Position of sample . . . . .	37
3.2.2. Reproducibility of measurements . . . . .	43
3.2.3. Sample's thickness resonances . . . . .	47
<b>4. Conclusion and way forward</b>	<b>52</b>
<b>Bibliography</b>	<b>53</b>
<b>Appendix</b>	<b>56</b>
A. Ultrasonic Spectroscopy "How to" guide . . . . .	57
B. Distance shift . . . . .	62
C. Position shift . . . . .	64
D. Reproducibility . . . . .	67

# 1. Introduction

Ultrasound refers to sound waves with a frequency of more than 20 kHz that are not audible anymore (Williams, 2012) and is a well known technique in diverse applications such as medicine (Fulgham, 2013; Maulik, 2005; Schrope and Goel, 2014), non-destructive testing (NDT) or food industry (McClements and Gunasekaran, 1997). Sending and receiving of transmitted or reflected ultrasonic pulses allows to obtain information about the sample under investigation and thus allows to detect flaws and irregularities or display images of the sample.

However, ultrasound measurements can also provide more throughout information about a material's properties and are thus used in physics and material sciences (Maynard, 1996). Taking the sample's resonance frequencies into account, elastic constants can be derived from the measurement. Álvarez-Arenas (2010) presented a method of ultrasonically measuring plant leaves and obtain their thickness, density, as well as velocity of sound and attenuation within the leaves. Recently Fariñas and Álvarez-Arenas (2015) presented a model that goes even further and allows an investigation of the layered structure of leaves.

As there exists a tight link between the leaves biological and ultrasonic qualities (Fariñas et al., 2014), that is especially sensible to the leaves water content (Álvarez-Arenas et al., 2009a,b; Sancho-Knapik et al., 2011), ultrasonic measurement methods provide a very promising tool for plant physiological and mechanical research. Working with air-coupled ultrasound is particularly interesting as this method allows a non-contact and non-contamination investigation of the sample (fig. 1). It can also be applied to living leaves for measurements over a longer period (Fariñas et al., 2014).



**Figure 1.:** Air-coupled ultrasonic measurement of a *Quercus muehlenbergii* leaf. (Sancho-Knapik et al., 2011)



**Figure 2.:** Ultrasonic wave that travels through a plate and forms internal reverberations within it. (us biomat)

The aim of this project is to design an experimental setup that allows the ultrasonic measurement of samples such as leaves to obtain their thickness, density as well as ultrasonic velocity and attenuation within them. Therefore, a detailed literature research has been carried out to gain an understanding on how this measurement method (called ultrasonic spectroscopy in this report) is carried out as well as on the complex data analysis involved in obtaining the material parameters.

The underlaying principle is the following: Usually if the ultrasonic wave hits an object, only part of the wave is transmitted through it to the receiver on the other side and the rest is reflected. As this procedure happens at the upper boundary as well as at the lower boundary of the object, multiple internal reflections form whithin the plate (fig. 2).

At a certain frequency however, the wavelength is exactly so that the internal reverberations constructively overlay and the transmittance is at its maximum: this is a thickness resonance of the sample. From the position of the thickness resonance ultrasonic as well as mechanical properties of the sample can be obtained. (Álvarez-Arenas, 2003a)

In the course of this work an experimental setup has been constructed that allows ultrasonic through transmission measurements under water. The set up has been characterized towards some of the main parameters that influence the measurements. Moreover some test measurements of a glass sample have been taken and processed to obtain the material properties. The results of the data analysis are not yet satifying, however the constructed setup provides enough flexibility to exploit and potentially provide measurements suitable to obtain the material properties.

## 2. Literature and theory

### 2.1. Basis

#### 2.1.1. Ultrasound

##### Ultrasonic wave

Sound is a form of mechanical energy, which travels through liquid or solid media as pressure wave. Sound waves are generated when an object vibrates in a medium. When the wave of sound energy propagates through the medium, alternating molecular compression and rarefaction occurs. However, although the molecules vibrate, they are not displaced.

In solids waves can propagate in four principal modes (fig. 3):

Longitudinal waves (= compressional waves = pressure waves)

Transverse waves (= shear waves)

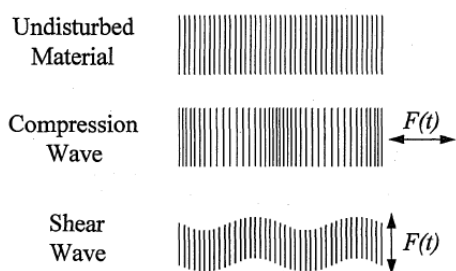
Surface waves (= Rayleigh)

Plate waves

In longitudinal waves, the oscillations occur parallel to wave propagation. Longitudinal waves can be generated in gases, liquids and solids. They are generated by an oscillating stress wave applied perpendicular to the surface of a material.

In transverse waves, the particles oscillate at a right angle to the direction of propagation. Transverse waves are effectively propagated in solid materials only. They are generated when the oscillating force is applied parallel to the surface of the material.

(Maulik 2005, McClements and Gunasekaran 1997, NDT)



**Figure 3.:** Wave propagation modes. Depending on the way the acoustic pressure  $F(t)$  is applied to the surface of the material, ultrasonic waves can propagate through materials as either compression or shear waves. (McClements and Gunasekaran, 1997)

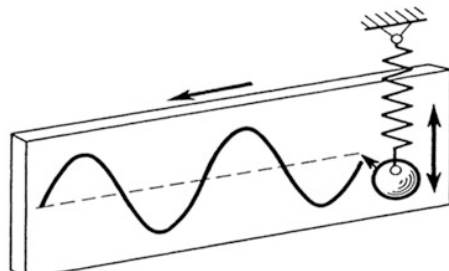


**Figure 4.:** Oscillation. The oscillation of particles as the wave propagates through the medium can be transformed into a displacement over time graph. (Magnus et al., 2013)

The wave can be described by different parameters. If the wave is plotted in a displacement against distance graph, the parameters wavelength  $\lambda$  (distance between two corresponding points on successive waves), amplitude  $a$  (maximum displacement from equilibrium position) and velocity  $v$  (velocity of energy moving through the medium) can be defined (fig. 4, 5). From a

graph of displacement against time, the wave's period  $T$  and frequency  $f$  can be derived as:

$$f = \frac{1}{T} \quad (1)$$

The frequency  $f$  is measured in Hertz (Hz: cycles per second, 1/s). "Ultrasound" refers to sound waves with a higher frequency than 20 kHz, that are not audible anymore. Instead of the frequency  $f$ , the angular frequency  $\omega$  can be used, with:

$$\omega = \pi f \quad (2)$$

Velocity  $v$ , frequency  $f$  and wavelength  $\lambda$  are related by:

$$v = f\lambda \quad (3)$$

Waves of identical frequency may start their oscillations simultaneously (in phase), or at different times (out of phase), described by the phase angle ( $\theta$ ).  
(Williams, 2012)

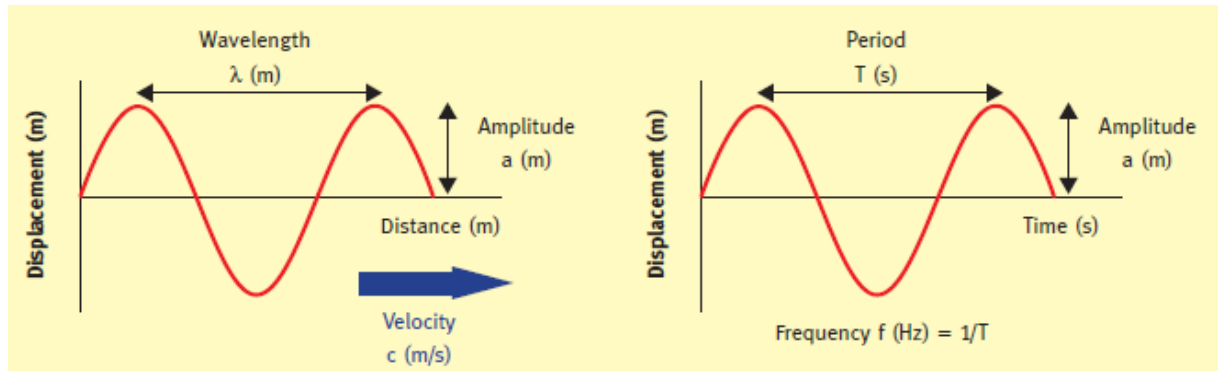


**Figure 5.:** Characteristics of waves. (Williams, 2012)

A wave or oscillation is called a harmonic oscillation if the displacement over time graph can be described with a sine or cosine function (whose argument is linear to time). Many oscillations that occur in nature or technique can be, at least approximately, described by a sine oscillation:

$$x(t) = x_m + a \sin \omega t \quad (4)$$

where  $x$  is the displacement and  $x_m$  the middle line ("zero-line"),  $a$  the amplitude ( $x_{max}$ ),  $\omega$  the angular frequency and  $t$  time. The oscillations can also be expressed in complex terms:

$$z = ae^{i\omega t} = a(\cos \omega t + i \sin \omega t) \quad (5)$$

To specify at which phase of oscillation (which "position") the oscillation is at the time  $t = 0$ , the phase angle  $\theta$  needs to be introduced in the term.

$$z = ae^{i(\omega t - \theta_0)} \quad (6)$$

(Magnus et al., 2013)

### Ultrasonic properties

The materials through which the ultrasonic wave propagates can be characterized by different properties:

**Velocity of sound  $v$**  The speed of sound  $v$  (or  $c$ ) in [m/s] is the distance traveled by an ultrasonic wave in unit time. Ultrasonic velocity in a material is fixed for any (nondispersive) medium. In materials that are less dense and more resistant to deformation, the ultrasonic wave propagates faster. As the differences in the elastic moduli (defining the resistance to deformation) of the materials are usually greater than those in density, the ultrasonic velocity is more determined by the elastic moduli than by the density. Thus it is greater in solids than in fluids, even though they are less dense. In leaves, that have a spongy mesophyll layer with high porosity, the velocity is expected to be very low (Álvarez-Arenas et al., 2009b; McClements and Gunasekaran, 1997). Exemplarily values for the velocity of sound in different materials can be found in tab. 1. However, the velocity of a wave can also be a function of its frequency or wavelength, then the propagating medium is a dispersive medium. Dispersion may be caused by the frequency dependence of the material, the scattering of waves due to fine inhomogeneities, the absorption or dissipation of wave energy. If a pulse propagates in a dispersive medium, it does not retain its initial shape. A short-duration pulse may be dispersed into wave trains in time. (Sachse and Pao, 1978)

The phase velocity of a (transverse) wave is the velocity with which planes of equal phase (e.g. a crest) progress through a medium. A number of waves of different frequencies however may be superposed to form a group that travels at the waves group velocity. The group would disperse with time because the wave velocity of each component would be different in all media except free space. (Pain, 2005)

In broadband-pulse technique, the phase velocity is inferred (Sachse and Pao, 1978). In this project dispersive materials such as leaves are used, therefore the frequency dependent phase-velocity is considered.

**Table 1.:** Acoustic properties of different materials

Material	Velocity of sound [m/s]	Impedance [rayl]	Ref.
Bone	3000-4500	$7.8 \times 10^5$	[1], [2]
Soft body tissues	1540	$1.58-1.70 \times 10^5$	[3], [4]
Air	330	400	[5], [6]
Water	1482.3	$14.5 \times 10^5$	[7], [8]
<i>Phormium tenax</i> leaf spongy mesophyll epidermis and chlorenchyma	450 560		[9] [10]

## References

- [1], [5] Schrophe and Goel 2014
- [2], [3], [4] Maulik 2005
- [6], [8] Pain 2005
- [7] McClements and Gunasekaran 1997
- [9], [10] Fariñas and Álvarez-Arenas 2014

**Pressure Amplitude  $p$**  The maximum value of variation in pressure generated by the propagation of a sound wave is called pressure amplitude  $p$  [Pa]. It can be measured with a transducer that transfers the pressure into a voltage signal [V].

**Power  $P$**  The rate of flow of ultrasonic energy (through the cross sectional area of the beam); energy per time [W].

**Intensity  $I$**  The rate of flow of ultrasonic energy per unit of cross sectional area, thus power per area; energy per time per area [W/m<sup>2</sup>].

The intensity is proportional to the square amplitude:

$$I \propto p^2 \quad (7)$$

The pressure amplitude of a sound wave is measured (e.g. by a hydrophone). A logarithmic scale is employed: the unit Decibel (dB). It describes the ratio of two measurements, for example the measurement of a transmitted sound wave with and without an obstacle in the wave propagation path. In dB, the ratio between the intensity of two measurements is given by (with eq. 7):

$$dB_{intensity} = 10 \log \frac{I_2}{I_1} = 10 \log \frac{(p_2)^2}{(p_1)^2} = 20 \log \frac{p_2}{p_1} = 20 \log \frac{[V_2]}{[V_1]} \quad (8)$$

(Maulik 2005, NDT)

In acoustics a common reference level for the sound pressure is a baseline of 20  $\mu\text{Pa}$ . A measured sound pressure  $p$  in Pa can thus be expressed in decibel by referencing it to 20  $\mu\text{Pa}$  as:

$$\text{Sound pressure level} = 20 \log_{10} \frac{p}{20 \mu\text{Pa}} \text{ dB} \quad (9)$$

Depending on whether a pressure amplitude ratio or a power ratio is considered, the decrease or increase of dB differs. For example if the power ratio is doubled, dB increases ca. 3 dB and decreases -3 dB if it is halved. The amplitude ratio however increases ca. 6 dB. (Parker, 2010; Schrope and Goel, 2014)

$$\begin{aligned} 3.01 \text{ dB}_{power} &= 10 \log \left( \frac{2}{1} \right) \\ -3.01 \text{ dB}_{power} &= 10 \log \left( \frac{1}{2} \right) \\ 6.02 \text{ dB}_{voltage} &= 20 \log \left( \frac{2}{1} \right) \end{aligned}$$

**Attenuation coefficient  $\alpha$**  The intensity of sound decreases exponentially with distance from the source, this phenomenon is called attenuation. Attenuation occurs mainly due to diffraction (= scattering) and absorption (see Interaction of waves). It is greater at high frequencies and in light, compressible media. The extend to which a material attenuates the ultrasonic wave is quantified in the attenuation coefficient, measured in [dB/m] or Nepers per meter [Np/m] (1 Np = 8.686 dB) and defined by:

$$A = A_0 e^{-\alpha x} \quad (10)$$

Where  $\alpha$  is the attenuation coefficient,  $A$  the amplitude of the wave,  $A_0$  the initial amplitude and  $x$  is the distance the wave has traveled through the material. (McClements and Gunasekaran, 1997; Williams, 2012)

**Acoustic impedance  $Z$**  The acoustic impedance of a medium is its resistance offered to sound transmission. It determines the fraction of an ultrasonic wave that is reflected from its surface. The specific acoustic impedance is given as

$$Z = \frac{\omega \rho}{k} \quad (11)$$

with angular frequency  $\omega$ , density  $\rho$  and wavenumber  $k$  (see below). In general  $Z$  is complex. But for materials where the attenuation of ultrasound is small (i.a.  $\alpha \ll \omega/v$ ), the following holds true:

$$Z = v\rho \quad (12)$$

where  $Z$  is the *characteristic impedance*, given as the product of the medium's density  $\rho$  and the velocity of sound in the medium  $v$ , in the unit [rayl]. (Maulik, 2005; McClements and Gunasekaran, 1997)

**Wavenumber and wave vector  $k$**  The complex wave vector  $\tilde{k}$  is defined as

$$\tilde{k} = k - i\alpha \quad (13)$$

$$k = \omega/v \quad (14)$$

where  $\alpha$  is the attenuation coefficient and  $k$  the wave vector or wave number,  $\omega$  the angular frequency and  $v$  the velocity. If there is attenuation in the medium, the wave vector is complex. For nonattenuating media,  $k$  is simply the non complex wavenumber ( $\omega/v$ ). (Álvarez-Arenas, 2003b; Haines et al., 1978)

### Interaction of waves

Interaction of waves with one another: If two waves of identical frequency, amplitude and phase combine, a single wave with twice the amplitude results (constructive interference). If the waves are  $180^\circ$  out of phase, they cancel each other out (destructive interference).

Interaction of waves with their environment (fig. 6):

Refraction: bending

Reflection: bouncing off

Diffraction: scattering

Absorption: conversion of waves kinetic energy in heat energy.

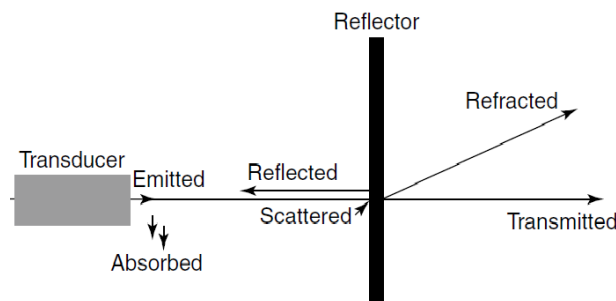


**Figure 6.:** Behavior of an acoustic wave as it travels through a medium. (Schrope and Goel, 2014)

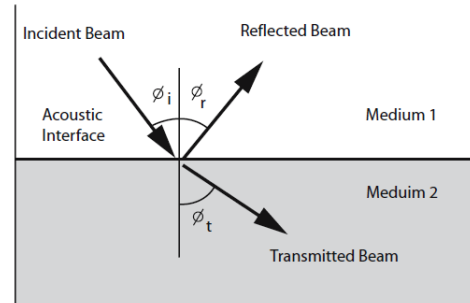


**Figure 7.:** Reflection, refraction and transmission of sound. The beam encounters the acoustic interface at an oblique angle of  $\Phi_i$ . A portion of the energy is reflected with the same angle  $\Phi_r$ . The rest is transmitted and refracted with an angle  $\Phi_t$  that depends on the angle of incidence and the velocity of sound in the two media. (Maulik, 2005)

Refraction occurs when a sound wave encounters an interface at an angle other than  $90^\circ$ . A portion of the wave is reflected and a portion transmitted. The direction of the transmitted waves is altered (refracted) (fig. 7).

Reflection occurs when a sound wave encounters an interface between two unlike media. From a large, flat surface, waves are reflected in a predictable way based on the incident angle (specular reflection). From small or irregular objects, the incident beam is echoed in different directions (diffuse reflection). Also, the scattering phenomenon can occur: When waves travel through a

medium and encounter reflectors whose size is much smaller than the wavelength of the propagating energy, a portion of the energy is then reflected in all directions in a spherical shape. The boundary between two media with different acoustic impedance is called an acoustic interface. At that interface, a certain amount of energy is reflected and the rest transmitted. The percentage of energy reflected is a function of the difference of the impedance of the tissues. If two adjacent tissues have a small difference in tissue impedance, very little energy will be reflected and most of it transmitted. If the impedance differences between tissues are very high, complete reflection of sound waves may occur.

(Fulgham, 2013; Maulik, 2005; Williams, 2012)

**Transmission coefficient** The transmission coefficient indicates which fraction of an incident wave is transmitted and which is reflected. A plane sound wave meeting at normal incidence an infinite plane boundary separating two media (fig. 8) is considered. On the one hand, the transmission coefficient for the transmission of pressure amplitude is given by the ratio of the amplitudes of the transmitted ( $A_{trans}$ ) to the incident wave ( $A_{inc}$ ). It is determined by the medias acoustic impedance  $Z_1$ , respectively  $Z_2$ :

$$\frac{A_{trans}}{A_{inc}} = \frac{2Z_1}{Z_1 + Z_2} \quad (15)$$

On the other hand, the transmission coefficient for the transmission of intensity is given by:

$$\frac{I_{trans}}{I_{inc}} = \frac{4Z_1Z_2}{(Z_1 + Z_2)^2} \quad (16)$$

(McClements and Gunasekaran, 1997; Pain, 2005)

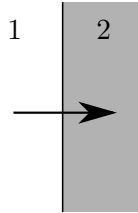


**Figure 8.:** Transmission of a wave at the boundary between two materials.

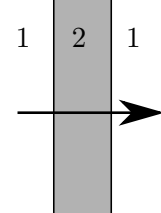


**Figure 9.:** Transmission of a wave through a material separating a medium.

For the transmission of sound through a solid material separating a fluid medium, the calculation that gives the transmission coefficient gets more complicated. The following case is considered: a homogeneous and isotropic plate and a one-dimensional monochromatic wave that travels through a surrounding medium 1, hits the plate (medium 2) at normal incidence, and is partly transmitted through to the same surrounding medium 1. (fig. 9)

The transmission coefficient as the amplitude ratio of transmitted to incident wave potentials is given by:

$$\frac{\tilde{A}_{trans}}{A_{inc}} = -\frac{2Z_1Z_2}{2Z_2Z_1 \cos k_2 t + i(Z_1^2 + Z_2^2) \sin k_2 t} = \xi \quad (17)$$

$$k_2 = \frac{\omega}{v_2} \quad (18)$$

With the acoustic impedance  $Z$ , the thickness of the plate  $t$  and the wavenumber  $k$ ; given by the angular frequency  $\omega$  and the velocity of sound (in the plate)  $v_2$ .  $A_{trans}$  is a complex amplitude because incident and transmitted waves are not in phase. (Álvarez-Arenas et al., 2009a; Fariñas and Álvarez-Arenas, 2015; Tempkin, 1981)

In relation to energy or intensities, the transmission coefficient as the ratio of transmitted-to-incident intensities (or the ratio of transmitted to incident energy fluxes) is given by:

$$\frac{|\tilde{A}_{trans}|^2}{A_{inc}^2} = \frac{4}{4 \cos^2 k_2 t + (Z_1/Z_2 + Z_2/Z_1)^2 \sin^2 k_2 t} \quad (19)$$

(Álvarez-Arenas et al., 2009b; Tempkin, 1981)

### 2.1.2. Ultrasonic transducers

An ultrasonic transducer converts electrical energy into mechanical energy (mechanical sound wave) and vice versa. In order to do so, the transducers use a piezoelectric crystal. The piezoelectric effect occurs when an alternating current is applied to a crystal containing dipoles (fig. 10). The areas of charge are distributed in a pattern within the piezoelectric element that has thus a “net” positive and negative orientation. When an alternating charge is applied to the two charged faces, an expansion and contraction of the material is obtained, resulting in a mechanical wave that is transmitted into the surrounding medium, usually through a coupling medium like gel. Hence, electrical pulses are converted into longitudinal sound waves. The other way around, an electric current is generated when a mechanical wave strikes the crystal. (Fulgham, 2013)

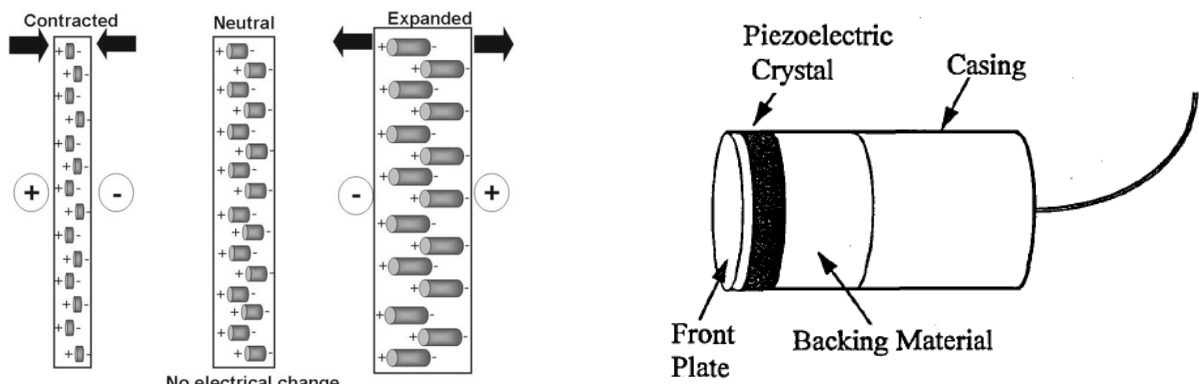


**Figure 10.:** Piezoelectric effect. Areas of “net” charge within a crystal expand or contract when a current is applied to the surface, creating a mechanical wave. (Schrope and Goel, 2014)

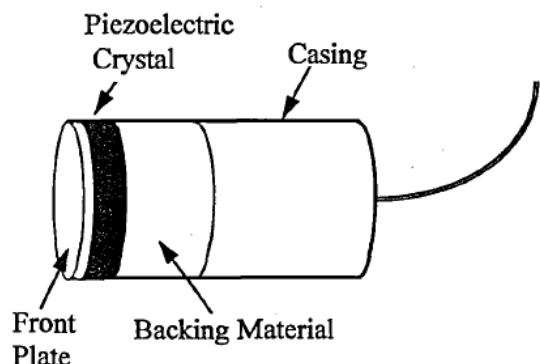


**Figure 11.:** Design of a piezoelectric transducer. (McClements and Gunasekaran, 1997)

The ultrasonic transducer consists of the piezoelectric crystal (usually made from either quartz or a ceramic such as lithium niobate) in a protective metal casing (fig. 11). The crystal is usually bonded to a front plate and a backing material. The backing material damps oscillations. The front plate is chosen so as to optimize the energy output of the transducer. Three important factors must be considered when choosing a suitable transducer: The range of frequencies it is capable of generating, its acoustic matching and its diameter.

**Frequency range of transducer** The range of frequencies a given transducer can generate depends on the resonant frequency of the transducer (the thicker the piezoelectric crystal, the lower the resonant frequency) and the degree of damping of the piezoelectric crystal (undamped transducer = narrow range of frequencies, centered around the resonance frequency).

A *broadband* transducer is a transducer that contains a highly damped crystal. When it is excited, the crystal produces a very short duration pulse that generates a wide range of frequencies centered near the resonant frequency.

**Acoustic matching** Usually the transducer is manufactured with a thin epoxy or ceramic wear-plate in front of the piezoelectric crystal. By varying the material of the wear-plate and its thickness, it is possible to acoustically “match” the transducer to a particular material, i.e. optimize the transmission of ultrasound from the transducer to the material. Most transducers are matched to either steel or water. (McClements and Gunasekaran, 1997)

**Anatomy of the ultrasound beam** The ultrasonic wave does not travel through a material with a diameter equal to that of the transducer that generated it. In practice, the ultrasonic beam spreads, that is known as (ultrasonic) diffraction or divergence.

An ultrasound beam consists of two regions: the near field (Fresnel zone) and the far field (Fraunhofer zone) (fig. 12). The near field has a converging beam profile. Since the beam originates from a number of points along the transducer face, the ultrasound intensity is affected by a complex pattern of constructive and destructive wave interference. At the end of the near field, the waves combine to form a relatively uniform front.

The far field has a divergent beam profile which results in a loss of ultrasound intensity.

At the point of transition between these zones, the maximal signal intensity is located and the wave is well behaved. The distance from the transducers face to that point ( $N$ ) is known as the focal distance or “natural focus” of a flat (unfocused) transducer.

For a piston transducer (a round transducer) of diameter  $d$ , a frequency  $f$  and a velocity  $v$  in a liquid or solid medium, the transition point  $N$  between near field and far field can be calculated as:

$$N = \frac{d^2 f}{4v} = \frac{d^2}{4\lambda} \quad (20)$$

The transducer beam spread in the far field occurs due to diffraction effects. The vibrating particles of the material through which the wave is traveling do not always transfer all of their energy in the direction of wave propagation, but also off at an angle.

The beam strength is always greatest at the center of the beam and diminishes as it spreads outward. It is greater for low frequencies and high transducer diameters. For a round transducer an approximation of the beam spread can be calculated as follows: The beam divergence angle  $\theta$  (1/2 the beam spread angle) represents the measure from the center of the acoustic axis to the point where the sound pressure has decreased by one half (-6 dB) to the side of the acoustic axis in the far field (fig. 12). Depending on the transducers diameter  $d$ , the sound velocity  $v$  and the frequency  $f$ , it is given by:

$$\sin \theta = 1.2 \frac{v}{df} \quad (21)$$

(Schrope and Goel 2014, McClements and Gunasekaran 1997, NDT)

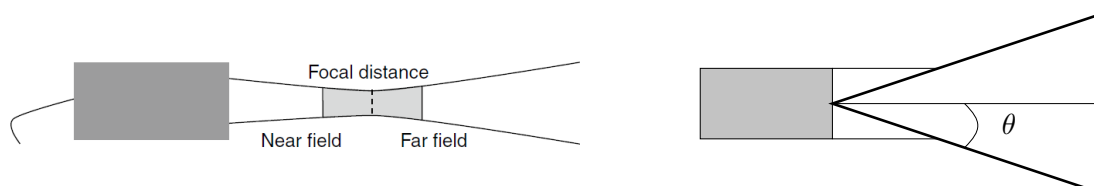


**Figure 12.:** Anatomy of an ultrasound beam. *Left:* Focal distance of a round transducer (Schrope and Goel, 2014). *Right:* Beam divergence angle  $\theta$ .

Other than the transducer, a signal generator is an important component of the ultrasonic measurement system. The signal generator creates the electrical input to a transducer. Frequency, amplitude and duration of the input signal must be chosen by the experimentator. The frequency content should correspond to the range of frequencies that the transducer is capable of generating. The type of the electrical input depends on the particular application: a sine wave with single frequency and infinite duration is used for continuous wave experiments, a short duration pulse which contains a wide range of frequencies is used for pulsed Fourier transform experiments and a pulse containing a predetermined number of cycles is used for toneburst experiments.

Once the signal traveled through the sample and returns to the receiving ultrasonic transducer, it is converted to an analog electrical signal which can be displayed on an oscilloscope. Using an analog-to-digital converter, the signal is digitized.

(McClements and Gunasekaran, 1997)

### 2.1.3. Signal processing

The returning ultrasonic signal is converted by a receiving transducer into an electrical signal which is digitized by an analog-to-digital converter. Two important features of the analog-to-digital converter are its digitization rate and its amplitude resolution. The digitization rate is the number of points along a signal that are sampled every second. The sample needs to be digitized at a rate at least twice the highest frequency component of the signal being analysed. The amplitude resolution determines how precisely the amplitude of the analog signal can be reproduced (typically 8 bits).

Once digitized, various signal processing techniques can be applied to the signal. For example averaging a number of signals to improve the signal-to-noise ratio. Also, digital smoothing can be used to remove high frequency noise (replacing each point of the received signal with an average of itself and its nearest neighbors). To remove frequency components not associated with the signal of interest, the signal can be filtered above and below certain frequency cutoff points. Cross-correlation techniques can be used to determine the time interval between two echoes.

The resulting signal of an ultrasonic experiment is usually in the time domain, i.e. amplitude vs. time. By using the Fourier transformation, the signal can be transformed into its frequency domain to show the frequency content of the signal. The underlying principle is that a signal in the time domain can be represented as a series of sine waves of different frequency, magnitude and phase.

From the measured phase and magnitude at each frequency, the frequency dependence of the ultrasonic velocity and attenuation coefficient can be calculated. Using a broadband pulse and analysing it in the frequency domain, the ultrasonic properties of a material can be measured over a range of frequencies using a single ultrasonic pulse. (McClements and Gunasekaran, 1997)

For more detailed information about signal processing, the following book provides a good start for beginners:

Parker, M. (2010). *Digital Signal Processing. Everything you need to know to get started.* Elsevier Inc., Burlington

To learn more about the Fourier Transform and how to do it in MATLAB, I used the following tutorials and help pages:

<http://www.thefouriertransform.com/>

<http://www.gaussianwaves.com/>, for example: <http://www.gaussianwaves.com/2015/11/interpreting-fft-results-complex-dft-frequency-bins-and-fftshift/>

<http://uk.mathworks.com/help/signal/ref/angle.html>

## 2.2. Ultrasonic measurement techniques

### 2.2.1. (Conventional) ultrasound techniques

**Pulsed techniques** Pulsed techniques include pulse-echo technique and through transmission technique. An electromagnetic pulse (with appropriate frequency, amplitude and duration) generates a short train of ultrasonic vibrations which travel across the sample, and the echoes are analysed. Velocity is determined from the time of flight and attenuation is determined from the decay of the echo amplitude with time.

In a through transmission setup, one transducer is used as a generator and a second one as a receiver. The sample is placed in between the transducers and a wave is generated that propagates through the sample.

In a pulse-echo setup the transducer launches an ultrasonic pulse that propagates through the sample until it reaches the far wall of the measurement cell, where it is reflected back to the transducer which also works as receiver. Because each pulse is only partly transmitted and partly reflected at the cell walls, a series of echoes is observed on the oscilloscope (fig. 13, 14).

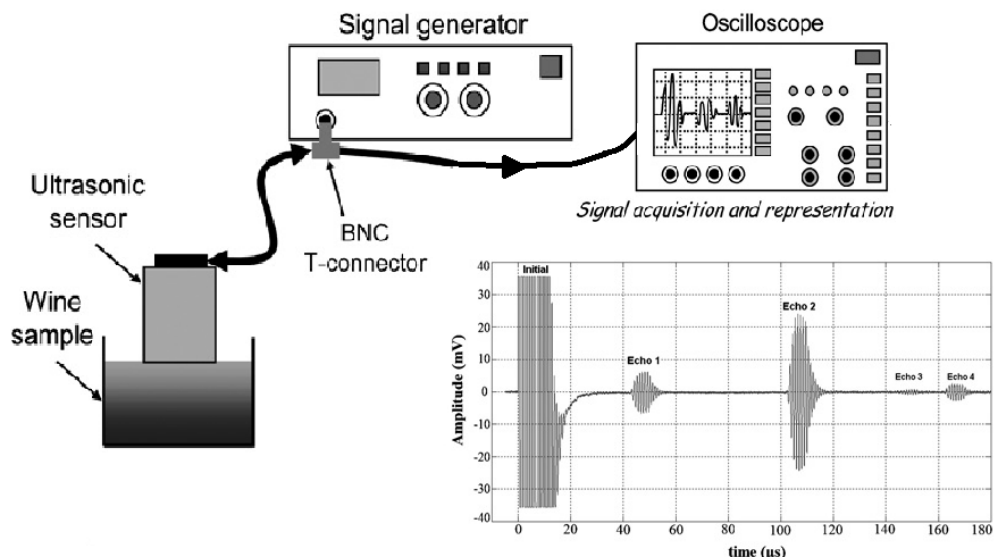


**Figure 13.:** Experimental setup for a pulse-echo experiment investigating a wine sample, showing the transmitted signal and received echoes. (slightly changed from Novoa-Díaz et al. (2012))

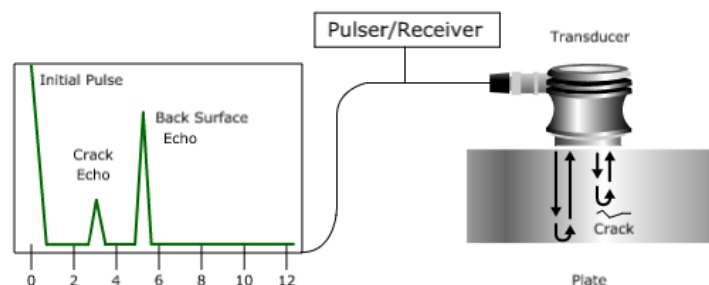


**Figure 14.:** Experimental setup for a pulse-echo experiment used for flaw detection. (NDT)

The first wave (“initial”) in fig. 13 corresponds to the excitation wave. The wave travels then through the front layer of the transducer and is partly reflected at the interface between front

layer and liquid and returns to the transducer as echo 1. The transmitted signal travels through the liquid, is reflected at the bottom of the measurement cell and returns to the transducer as echo 2. The time elapsed between the arrival of echo 1 and echo 2 is the time taken by the ultrasonic wave to travel a distance of  $2d$  through the liquid, the time-of-flight (with  $d$  = distance liquid surface to bottom). The echoes 3 and 4 are subsequent multiple reflections of echo 2 at the transducer and at the interface between front layer and liquid. Those echoes will always reach the transducer after the arrival of echo 2, without interfering with the measurement in question.

The ultrasonic velocity is determined from the time-of-flight (TOF), which is the time it takes an ultrasonic wave to travel from the transmitter to the receiver transducer (which in a pulse-echo setup are the same). If the distance  $d$  travelled by an ultrasonic wave is constant its velocity  $c$  can be calculated from the TOF by

$$c = \frac{d}{TOF} \quad (22)$$

If the ultrasound measurements are used to monitor processes or characterize changes that occur in a medium (such as fermentation of food), the TOF variations over a certain period of time are measured. There are different methods to calculate the TOF-variations between signals, such as the threshold method. Here the TOF is estimated as the time at which the amplitude of the ultrasound signal at the receiver first exceeds a preset threshold. Its main limitation is that the TOF is overestimated since the threshold level must be high enough to eliminate false detections. Other methods are the maximum detection method, the zero-crossing method and the cross-correlation method. These are all time domain methods. In the frequency domain, there is the phase-shift and phase-slope difference technique.

(McClements and Gunasekaran, 1997; Novoa-Díaz et al., 2012)

**Continuous wave techniques** A similar setup like the one for a through transmission experiment is used, but the transducer is driven continuously. At frequencies corresponding to the sample length being some multiple of a half-wavelength of sound, resonant responses are observed. From the measured resonant frequencies, the wave velocity is determined and attenuation is determined from the Q-factor of the resonance lines. (Leisure and Willis, 1997)

Another application of continuous wave ultrasound is a measurement device called interferometer (see McClements and Gunasekaran (1997) for details).

**Applications of ultrasound techniques** Ultrasonic methods are used in various fields. Medical applications include for example gynecology and urology. Also, ultrasonic testing is an important nondestructive testing method, used in industrial inspections, that allows to locate and characterize material conditions and flaws (e.g. fig. 14) (NDT). Other than that, ultrasonic measurements are applied in the food industry because they provide information about the physicochemical properties of food (composition, structure, flow rate, physical state, molecular properties) (McClements and Gunasekaran, 1997).

Furthermore, ultrasound techniques are used in physics and material sciences. The ultrasound velocity provided by the measurements (eg. by time-of-flight measurements with pulses) allows a very accurate characterization of the elasticity of solids. From the velocity, the elastic constants of the material can be derived.

But the above mentioned usual testing methods have several disadvantages. The interpretation of results (to obtain the elastic constants) relies on the assumption of a plane wave and therefore large samples are required. Although the wave near the transducer is approximately planar, diffraction effects exist. Also, the bonding of a transducer face to the sample can have negative effects. Finally, to determine the complete set of elastic constants, a number of independent

measurements must be made and often separate samples are needed.

*Resonant ultrasound spectroscopy* is an alternative technique, that drastically reduces the amount of material required for accurate results. The elastic properties may be fully characterized by one spectrum on one sample. Furthermore, the accuracy of this method is high and it does not rely on a plane-wave approximation. This technique can be applied to any well defined sample shape and to materials with any crystallographic symmetry.

(Leisure and Willis, 1997)

### 2.2.2. Resonant Ultrasound Spectroscopy (RUS)

RUS is based on the measurement of the vibrational eigenmodes (natural resonance frequencies) of samples of well defined shapes. From the RUS-measurement of the (usually mineral) samples, the elastic constants of the material are determined. The sample is held lightly between two piezoelectric transducers (no bonding, stress-free boundary conditions, minimization of loading) (fig. 15). The sample is excited at one point by one of the transducers. Instead of an approximation to plane waves, a continuous wave excitation at a tunable frequency is used. The frequency of the driving transducer is swept through a range, corresponding to a large number of vibrational eigenmodes of the sample. A large response is observed when the frequency of the driving transducer corresponds to one of the sample's eigenfrequencies. If the configurations are right, enough eigenfrequencies are observed to determine all elastic constants from one measurement. The eigenfrequencies depend on the elastic constants, sample shape, crystallographic orientation and density. Usually sample shape, crystallographic orientation and density are known and one can determine the complete elastic constant matrix from such a spectrum.

But although the RUS spectrum contains much information, it is complicated to extract it all. The procedure to find the elastic constants is the following: The measured frequencies are compared with the computed frequencies which are calculated with an initial set of input parameters. Those are varied in an iterative process. The forward problem consists of calculating the natural frequencies from elastic constants and sample shape. To find the elastic constants from the measured natural frequencies (the inverse problem) a nonlinear inversion algorithm is applied. It starts with a guessed set of elastic constants and uses an iteration procedure to find the set of constants that fits best to the measurements (usually in a least square sense).

(Leisure and Willis, 1997; Maynard, 1996)

More details can be found in:

Migliori A. and Sarrao J. (1997). *Resonant Ultrasound Spectroscopy. Applications to Physics, Materials Measurements, and Nondestructive Evaluation.* John Wiley & Sons, Inc., New York

### 2.2.3. Broadband ultrasonic spectroscopy

In a broadband pulse, the ultrasonic energy is spread out over a wide range around a particular frequency. The broadband transducer produces a very short duration pulse, that generates a wide range of frequencies centered near its resonant frequency. (McClements and Gunasekaran, 1997)

In broadband ultrasonic spectroscopy, these broadband pulses are transmitted through or reflected from a sample. By using the Fourier transform, the frequency domain (frequency dependence of amplitude and phase information) is then analysed. As a result, frequency, velocity, and attenuation of ultrasonic waves in materials can be measured. This technique can also be applied to dispersive materials, like plant leaves for example, and to thin materials. (Sancho-Knapik et al., 2010)

Broadband ultrasonic spectroscopy was used by Sachse and Pao (1978) to determine phase and

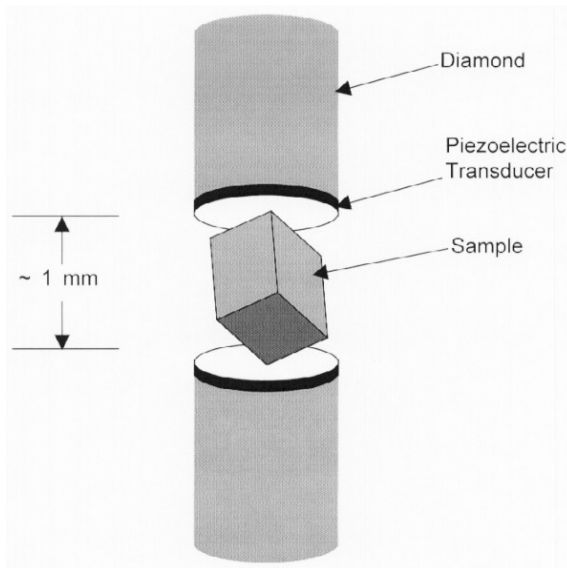


**Figure 15.:** Experimental setup for Resonant Ultrasound Spectroscopy (RUS). (Leisure and Willis, 1997)

group velocities of dispersive waves in solids, by analysing the phase spectrum. Haines et al. (1978) used broadband ultrasonic spectroscopy to study layered media. Reflected pulses are analysed in the complex frequency domain which gives information on amplitude and phase spectra. Measurement of the phase change as a function of frequency is used to determine acoustic parameters (velocity, impedance, attenuation) of the layered material.

Broadband spectroscopy technique was applied to plant leaves by Fukuhara (2002). By comparing the phase and magnitudes when moving the leaves in and out of the acoustic pathway, the phase velocity, frequency and attenuation coefficient of the samples were determined.

For the experiments carried out by Haines et al. (1978) and Fukuhara (2002), the transducers need a liquid coupling in order to transmit the ultrasonic waves. Also, the measurements do not rely on the excitation and analysis of resonance frequencies.

#### 2.2.4. Air-coupled ultrasonic spectroscopy ("Non-Contact RUS")

Air-coupled ultrasonic spectroscopy is an application of broadband ultrasonic spectroscopy to the measurement of materials without immersion of the sample in water or using coupling fluids. That is possible thanks to the development of new broadband ultrasonic emitters and receivers that can transmit and receive signals to and from any gas. (Sancho-Knapik et al., 2010)

As in RUS, there are resonances analyzed. But for very soft materials or for plate samples, a conventional RUS experimental setup (transducers need point contact with sample) is not possible. Instead, air-coupled ultrasound is used. With air-coupled ultrasound technique, thickness resonances of plates are excited and sensed to obtain elastic constants (in this sense the technique is a non-contact RUS). (us biomat)

For this project only water coupled transducers were available. Thus ultrasonic measurements were carried out under water but with the same aim: To excite and sense thickness resonances of the sample and use these to characterize the material tested.

## 2.3. Ultrasonic Spectroscopy

### 2.3.1. Overview

Procedure

- *Measure:* the transmitted pulse in the time domain and analyze via FFT the phase and amplitude spectra with resonance frequencies (thickness resonances)
- *Aim:* to obtain thickness and density of sample as well as velocity of sound and attenuation in the sample.

Compared to former analysis, the procedure explained below in more detail (Álvarez-Arenas, 2010), has the advantage that the thickness of the plate (sample) needs not to be measured separately but can also be obtained by the ultrasonic measurement. Therefore, the method can be applied also to materials where an independent thickness measurement is not possible, like soft membranes or biological samples (e.g. drying vegetable samples that change thickness in progress).

Both amplitude and phase spectra of the transmission coefficient are measured simultaneously. By the analysis of the spectra of the first order resonance, it is possible to derive the effective mechanical properties of the sample (e.g. a leaf) in the direction normal to the leaf plane. (Fariñas and Álvarez-Arenas, 2014)

Advantages of ultrasonic spectroscopy (Álvarez-Arenas, 2003a,b)

- No contact, no contamination
- Rapid inspection (online, real-time)
- Information about surface, whole volume and back of surface
- Testing can be over a bigger surface or focused at single point (depending on transducer type)
- Can be applied to dispersive materials

For broadband ultrasound spectroscopy in general, the experimental setup can be either a pulse-echo setup (e.g. Haines et al. (1978)), or a through-transmission setup. However, the proceedings here explained are for a through-transmission setup.

The sample is put in between two transducers, an emitter and a receiver. The incident wave is partly reflected and partly transmitted at the interface of surrounding medium and sample (fig 16). The transmitted wave propagates and reaches the back surface, where again a part of the energy is reflected and a part transmitted. The transmitted wave travels through the surrounding medium to the receiver transducer and arrives with a phase shift and frequency shift. This process is repeated for each of the multiple internal reflections in the plate (reverberations). (Álvarez-Arenas, 2003a)

The transmitted signal is compared to the signal of reference (= the incident signal, measured without the sample in between the transducers) (fig. 17) First, the signal without the sample is measured and the FFT calculated (amplitude  $A_0(\omega)$  and phase  $\phi_0(\omega)$ ). Then the sample is put between the transducers, the signal is measured and the FFT calculated to get amplitude  $A(\omega)$  and phase  $\phi(\omega)$ . The phase shift induced by the transmission through the plate, depending on the frequency, is obtained (phase spectra of the transmission coefficient) and the change of amplitude (magnitude spectra).

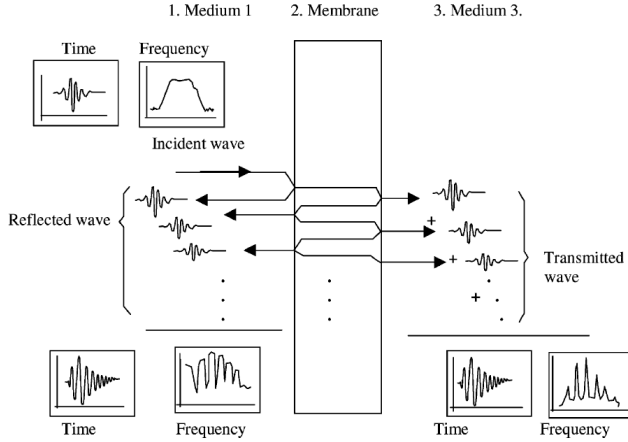


**Figure 16.:** Schematic illustration of sound transmission through a plate and multiple reverberations within it. (Álvarez-Arenas, 2003a)

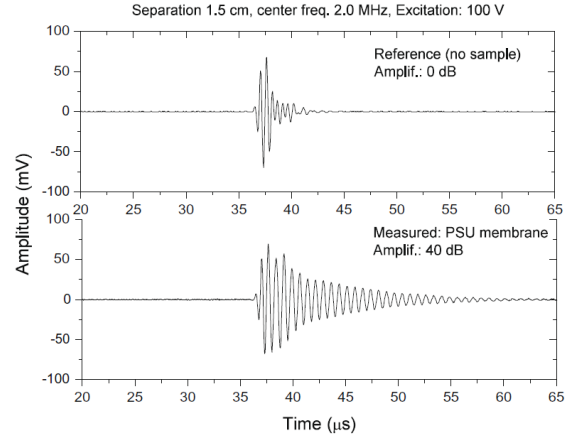


**Figure 17.:** Transmitted signal from transmitter transducer to receiver in the time domain. *Up:* reference signal without sample. *Down:* transmitted signal through a PSU membrane. Measured with air-coupled transducers. (Álvarez-Arenas, 2010)

The phase spectra of the transmission coefficient is calculated as follows:

$$\text{Phase shift } \Delta\phi = \phi(\omega) - \phi_0(\omega) \text{ [rad]} \quad (23)$$

The magnitude spectra of the transmission coefficient is the frequency dependent magnitude of the transmitted waves amplitude pressure  $A(\omega)$  in relation to the incident waves amplitude pressure  $A_0(\omega)$  (see eq. 18), given by:

$$\xi = \frac{A(\omega)}{A_0(\omega)} \text{ [V]} \quad (24)$$

Moreover, the transmission coefficient in relation to intensities is given by  $A(\omega)^2/A_0(\omega)^2$  (see eq. 19). (24) is also called the *insertion loss* and can be transferred to the unit [dB] as follows (see eq. 8):

$$\text{Insertion loss } IL = 20 \log(A(\omega)/A_0(\omega)) \text{ [dB]} \quad (25)$$

(Álvarez-Arenas, 2003a, 2010; Álvarez-Arenas et al., 2009b)

Alternatively, the measured amplitudes in [V] can be first transferred to [dB] by comparing them to a reference value  $A_{ref}$ . This gives the amplitude or magnitude  $I$  in [dB]. The insertion loss (= magnitude of transmittance) is than given by the difference.

$$\text{Magnitude } I(\omega) = 20 \log(A(\omega)/A_{ref}) \quad (26)$$

$$\text{Magnitude } I_0(\omega) = 20 \log(A_0(\omega)/A_{ref}) \quad (27)$$

$$\text{Insertion loss } IL = I(\omega) - I_0(\omega) = 20 \log(A(\omega)/A_0(\omega)) \quad (28)$$

$$\log(a/b) = \log(a) - \log(b)$$

(Sancho-Knapik et al., 2010)

Insertion loss and phase shift can then be plotted against the frequency (fig. 18). In the spectrum, *thickness resonances* can be observed (if the proper combination of transducer frequency band, ultrasound velocity in the material and plate thickness is given (see eq. 30)).

A thickness resonance of the sample occurs, when the maximum value of the transmitted energy is observed (maximum in magnitude-frequency plot). The occurrence of resonance frequencies can be explained as follows: The incident wave is partly reflected on the surface and again on the back surface (multiple internal reflections). Each of the multiple internal reflections goes through this process again, so that consecutive internal reflections arrive at the back surface. When the time-delay between them equals  $1/f$  (with  $f$  being the frequency of the wave), constructive interference takes place and the maximum value of the transmitted energy is observed (= total loss of energy inside the material). This is a thickness resonance of the sample. For the thickness resonances of a plate (one layer) separating two media, maximum values of transmission coefficient  $T$  (= thickness resonances) are located at:

$$f_n = n \frac{v}{2t}, \quad n = 0, 1, 2, \dots \quad (29)$$

$$\omega_n = n \frac{2\pi v}{2t} \quad (30)$$

with thickness  $t$  of plate, velocity  $v$ , resonance frequency  $f_n$  and angular resonance frequency  $\omega_n$ . The first thickness resonance ( $n = 1$ ) is located at

$$\omega_1 = \frac{2\pi v}{2t} \quad (31)$$

$$v = \frac{2\omega_1 t}{2\pi} \quad (32)$$

As for dispersive materials, such as leaves, the phase velocity depends on the frequency:

$$v(\omega_1) = \frac{2\omega_1 t}{2\pi} \quad (33)$$

(Álvarez-Arenas, 2003a,b, 2010; Fariñas and Álvarez-Arenas, 2015)

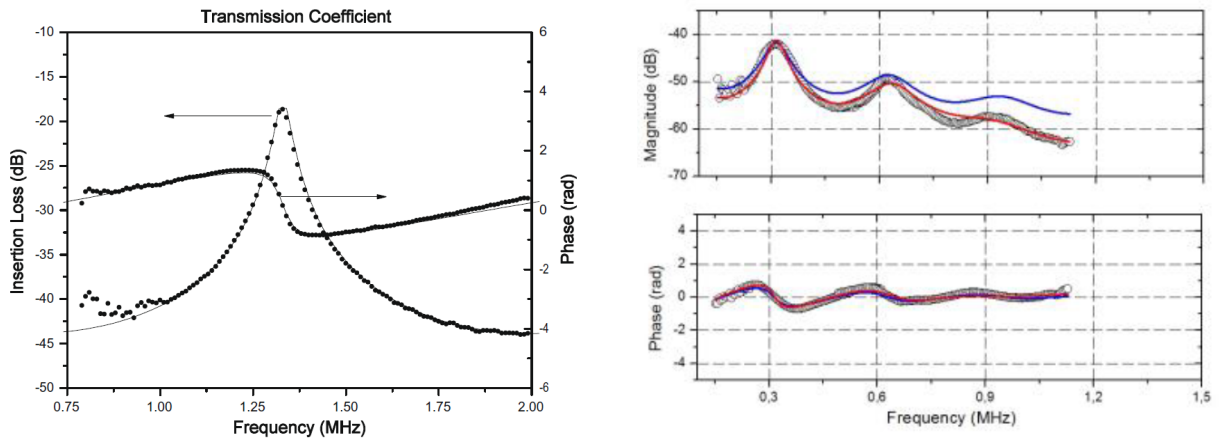


**Figure 18.**: Amplitude and phase shift spectra of the ultrasonic transmission coefficient of a polyethersulfone membrane (left) and a *Ligustrum* leaf (right). Dots show experimental data. The solid lines represent theoretical data, obtained by theoretical models explained in the following sections. From the plots it can be seen, that the maximum in the magnitude-frequency plot (thickness resonance) corresponds to the point of inflection in the phase spectra. Also, the second thickness resonance observed in the *Ligustrum* leaf is double the first as it can be obtained from eq. 30 with  $n = 2$ . (Álvarez-Arenas, 2010; Fariñas and Álvarez-Arenas, 2015)

From the phase and magnitude spectrum with thickness resonances, the aimed parameters (density, thickness, velocity and attenuation) can be obtained. This analysis has been carried out by the Ultrasounds for Biological Applications and Materials Science Group, that has kindly

provided their python code online. It contains a routine for the procedure explained in the following sections. That is to extract material properties of a plate (density  $\rho$ , thickness  $t$ , ultrasound velocity  $v$  and attenuation  $\alpha$ ) from the measured phase and magnitude spectra of the transmission coefficient. (us biomat)

The observed thickness resonances are needed to solve the inverse problem that occurs when using the measured spectra to obtain velocity, thickness of the material, its density and the attenuation coefficient. (See also *Inverse Problem*).

The transmission coefficient is theoretically modeled. To calculate the transmission coefficient, a-priori values (initial guess values, seeds) for  $v$ ,  $\rho$ ,  $t$  and  $\alpha$  are derived from the measurement. Even though they are derived from the measurements, due to assumptions and simplifications they are not entirely correct. Then the calculated transmission coefficient is fitted to the experimental results in order to find the best values for  $v$ ,  $\rho$ ,  $t$  and  $\alpha$ , i.e. those for that the calculated transmission coefficient shows the best coherence with the experimental results. This fitting routine is based on the Gradient Descent method and is implemented in the afore mentioned python script. The procedure is explained in more detail in the next section. See fig. 19 for an overview of ultrasonic spectroscopy.

### ***Inverse Problem***

“To predict the result of a measurement requires (1) a model of the system under investigation, and (2) a physical theory linking the parameters of the model to the parameters being measured. This prediction of observations, given the values of the parameters defining the model constitutes the “normal problem”, or, in the jargon of inverse problem theory, the forward problem. The “inverse problem” consists in using the results of actual observations to infer the values of the parameters characterizing the system under investigation.

Inverse problems may be difficult to solve for at least two different reasons: (1) different values of the model parameters may be consistent with the data (knowing the height of the main-mast is not sufficient for calculating the age of the captain), and (2) discovering the values of the model parameters may require the exploration of a huge parameter space (finding a needle in a 100-dimensional haystack is difficult). ”

(WolframMathWorld)

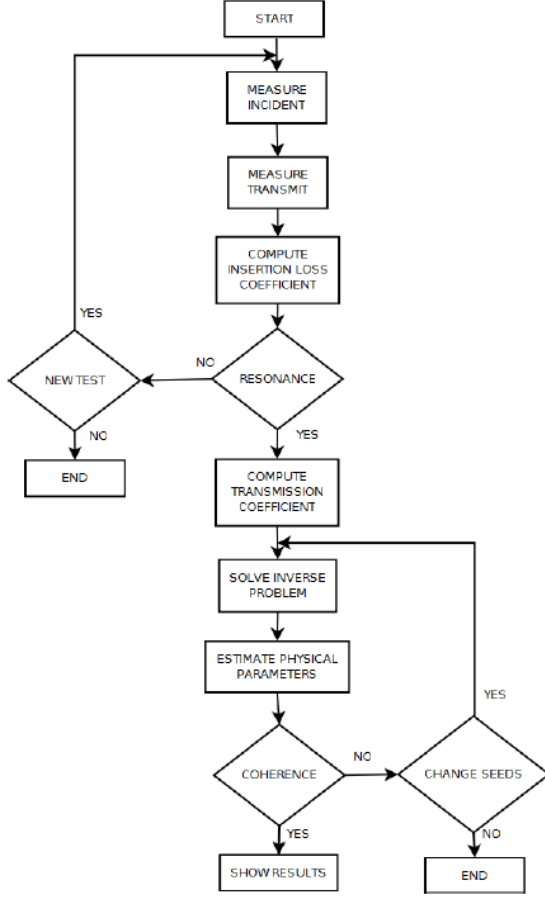


**Figure 19.**: Ultrasound spectroscopy technique. Transmitted and incident signals are compared and if resonances occur, the inverse problem associated with sound transmission in three media can be solved and the internal physical characteristics (velocity, thickness, density and attenuation) can be obtained. (Collazos-Burbano et al., 2014)

### 2.3.2. Modeling the transmission coefficient (one-layer model)

To model the transmission coefficient, a plane longitudinal wave at normal incidence is considered. The sample (e.g. a leaf) is considered a homogeneous, solid, flat plate. Even if leaves have a complex microstructure, the effective medium approach can be applied to solve the inverse problem associated with the transmission of sound waves in three media. Hence, the obtained parameters are effective leaf properties (see *Effective Properties*). (Álvarez-Arenas et al., 2009b; Fariñas and Álvarez-Arenas, 2014)

The following theoretical relations are used: The velocity of the sound wave in the plate  $v$ , if the reverberations inside the plate are negligible, is given by:

$$v(\omega) = \frac{t}{t/v_1 - \Delta\phi/\omega} \quad (34)$$

where  $t$  is the thickness of the plate,  $v_1$  the velocity in the surrounding medium,  $\Delta\phi$  the phase shift and  $\omega$  the angular frequency.

The presence of reverberations inside the plate modifies the situation (fig. 16). For the transmission through a plate, the transmission coefficient (amplitude ratio of transmitted to incident wave potentials  $\xi$  (eq. 18)) is then given by:

$$\xi = \frac{-2Z_1Z_2}{2Z_1Z_2 \cos(kt) + i(Z_1^2 + Z_2^2) \sin(kt)} \quad (35)$$

with the acoustic impedance  $Z$ , the thickness of the plate  $t$  and the wavenumber  $k$  (given by the ratio of the angular frequency  $\omega$  and the velocity of sound in the plate  $v_2$ ). This expression yields a complex magnitude, because transmitted and incident waves are not in phase. The reverberations within the plate cause a phase shift.

If the plate is at resonance however, that is when the resonance condition eq. 33 holds true,  $\xi$  becomes real valued (if dissipation in the plate can be neglected). Then, eq. 34 holds true even for a plate with reverberations within it. If the frequency of maximum transmission and the phase at that frequency are measured, eq. 33 and 34 can be solved for the two unknowns: velocity and thickness.

But dissipation takes place and the signal is attenuated inside the sample. That is not taken into account for by eq. 33 and 34. Therefore, the measured resonance frequencies are not those used in the calculation, but they are displayed away from those theoretical values. To account for that fact, eq. 35 is used and an attenuation factor  $\alpha$  is introduced in that equation by fitting the theoretically calculated resonance from 35 to the experimentally measured one. (Álvarez-Arenas, 2010)

When using eq. 35, the acoustic impedance  $Z$  appears, that is the product of velocity  $v$  and density  $\rho$  of the sample. A first value for  $v$  has already been obtained above, density is calculated from the minimum value of transmission coefficient. The attenuation coefficient at resonance ( $\alpha_{f_1}$ ) is calculated from the measured Q-factor at resonance. Thus, from the measurements approximate values for  $v, t, \rho$ , and  $\alpha$  are obtained. As explained above, these values are not completely correct, as they are obtained by equations that do not correctly represent the mea-

### **Effective Properties**

In elementary material mechanics, the materials are often considered as ideal rigid bodies that are homogeneous and possesses an uniform and regular internal structure. Therefore, the properties between the material and its components (e.g. between a gold brick and a gold crystal) do not really differ from one another. In the engineering world however, there are hardly such ideal materials but materials have to be treated as a composite system (e.g. a gold being a mixture of gold crystals, contaminations and pores). The correlation between the properties of the ingredients and the resulting products are rather weak. The components interact more or less with each other or may even be at different phase states. Therefore the analysis and prediction of behaviors of composites is quite complicate.

To cope with that complexity, the concept of effective properties is used. For the multi-component and/or multiphase complex material, its behaviors are dictated by each component. Its overall macroscopic property is therefore not equal to that of any single constituent, but rather a collective one contributed by all components. The *effective property* is actually the equivalent property of a hypothetical simple material (homogeneous, single component, single phase) which yields the same response as that of the complex one at the same given conditions. Because the different components and phases will behave different under different ambient conditions and external excitations, the complex system as well depends on these conditions and thus different equivalent simple systems are needed to represent the complex one.

The theoretical prediction of effective properties for multiphase material systems is very important for analysis and optimization of material performance, but also to design new materials.

(Wang and Pan, 2008)

sured spectra that is shifted away from the simple equations due to dissipation/attenuation effects.

These values for  $v$ ,  $t$ ,  $\rho$ , and  $\alpha$  are used to calculate the theoretical prediction for the transmission coefficient. The theoretical values are fitted into the experimental data by considering a power law for the variation of the attenuation coefficient with the frequency:

$$\alpha(f) = \alpha_{f_1} \times (f/f_1)^m \quad (36)$$

The values for  $v$ ,  $t$ ,  $\rho$ , and  $\alpha$  are introduced as initial guess in a fitting routine based on the Gradient Descent method, to find the set of leaf parameters  $v$ ,  $t$ ,  $\rho$ ,  $\alpha$  and  $m$  that minimize the error between the calculated transmission coefficient spectra and the measured one. (Álvarez-Arenas et al., 2009b; Fariñas and Álvarez-Arenas, 2015)

### 2.3.3. Limits of the one-layer approach and models for more layers

Considering the sample a flat homogeneous plate is often a simplification. Materials such as leaves possess a complex, layered structure (see *Leaf anatomy*) that alters the reverberations of ultrasound within it (fig. 20). For the material characterization of such complex materials, the ultrasound results may differ from the otherwise obtained results.

For example, if one compares density of leaves obtained by independent measurements and obtained by ultrasonic measurements, the ultrasonic measurements are biased towards higher values for density. This is due to the simplifications of the one-layered model: Density is worked out from the velocity of sound and the acoustic impedance of the leaf. The amount of energy that is reflected and transmitted at the leaves surface is determined by the acoustic difference between the leaf and the surrounding fluid. But the density of the leaf's surface is expected to be different from the density in the inner part. In the one-layered model however, from the transmission coefficient at the surface, the density is derived for the whole leaf and thus biased. Furthermore, internal reflections from the internal border between the layers are not account for by the one-layer model. This loss of energy is assumed to be produced at the leafs interface with the surrounding fluid by wrongly estimating a larger leaf density. (Fariñas and Álvarez-Arenas, 2014)

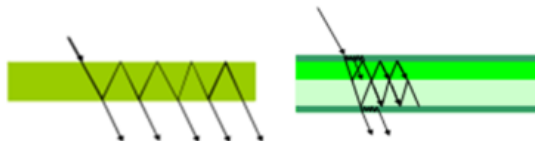


**Figure 20.:** Reverberations in a one-layer plate (*left*) and a layered plate (*right*). (us biomat)

Regarding the transmission coefficient spectrum, the one-layer modeling provides good results for a frequency range around the first thickness resonance, even though leaves are a complex, anisotropic and heterogeneous material. But when the leaves are measured at higher frequencies and resonances of higher orders are observed, the periodicity of the resonances is altered and is not well described by the theoretical model anymore (fig. 21). This deviation of higher resonance orders can be attributed to the layered structure of the leaf. As frequency increases, the resonance of sublayers may become more apparent, as well as the coupling between them. (Álvarez-Arenas et al., 2009b)

Therefore a layered model is introduced, which allows to obtain information about the different layers that constitute the leaf.

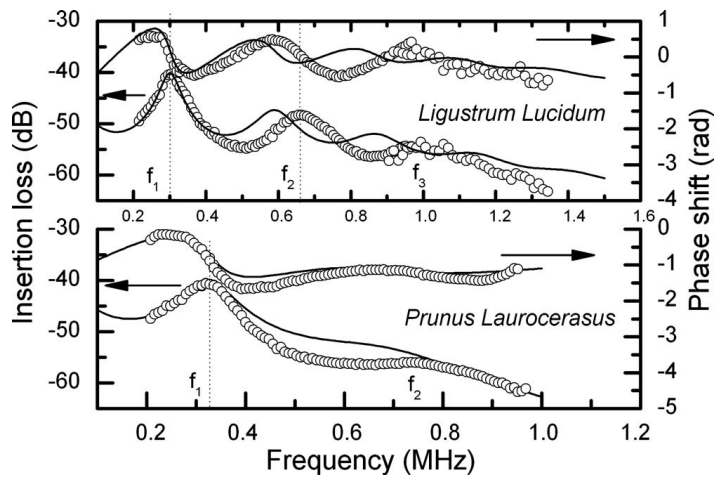


**Figure 21.**: Insertion Loss and phase shift vs. frequency for a *L. lucidum* and *P. laurocerasus* leaf. The solid line represents the theoretical one-layer model. In the vicinity of the first thickness resonance it fits well to the experimental data. At higher frequencies however, a frequency shift of the experimental data away from the theoretical one is observed, that is due to the layered structure of the leaf. (Álvarez-Arenas et al., 2009b)

### Leaf anatomy

A typical bifacial leaf consists of four layers (see figure): the upper epidermis, the palisade parenchyma, the spongy mesophyll and the lower epidermis. The epidermis is build by one tight cell layer without intercellular spaces. Contact with the environment is possible through special openings, so called stomata. Additional it may be covered by a cuticula, preventing water flow.

Palisade and spongy parenchyma contain a large amount of chloroplastes and are specialized in photosynthesis. The palisade parenchyma is quite dense and one to three layered with vertically orientated cells. It contains about 45% of the leaf's chloroplastes and functions as assimilating tissue. The spongy parenchyma is more loose and contains many, sometimes huge, intercellular spaces. It serves for the leaf's transpiration.

(Kadereit et al., 2014)

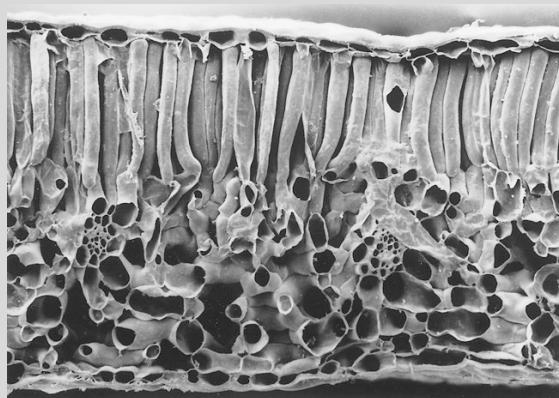


**Figure:** Cross-section through a leaf of *Helleborus foetidus* (100x). The layered structure is clearly visible. Also, in the spongy mesophyll, two vascular bundles are visible. (Kadereit et al., 2014)

## Two-layer model

Leaf samples can be simplified as two layer plates where one layer represents the upper epidermis and the palisade parenchyma and the other one the lower epidermis and the spongy mesophyll. When modeling a two layered system, the number of involved variables unfolds: thickness, density, velocity, attenuation and attenuation variation with frequency of each layer is required. The values obtained from the one-layer model, considering the leaf a homogeneous plate, are used as initial guess for a fitting routine based on the Gradient Descent method. The fitting routine is used to find the set of material parameters that minimize the error between the calculated and measured transmission coefficient. To do so an algorithm structured in two main loops is used: A first loop that varies velocities and densities (related to the location of the resonance peaks). And a second loop that varies the parameters related to attenuation (related to the variation of energy with frequency).

There are infinite solutions for the selected error minimization requirements. All solutions are equivalent from the point of view of significant parameters: the acoustic impedance and the wavenumber and thickness product. (Fariñas and Álvarez-Arenas, 2015)

Fariñas and Álvarez-Arenas (2015) used the two-layer approach on a number of different plant leaves. They showed that the difference in the ultrasonic response of the different leaves corresponded to the histological difference between them. The *Abelia* leaf in fig. 22 has a distinct layer of palisade parenchyma and highly porous spongy mesophyll. This strongly layered structure is not taken into account in the one-layer model. The position of the second resonance peak expected by the one-layer model is the double of the first one (maximum of the blue line in fig. 22, see eq. 30).

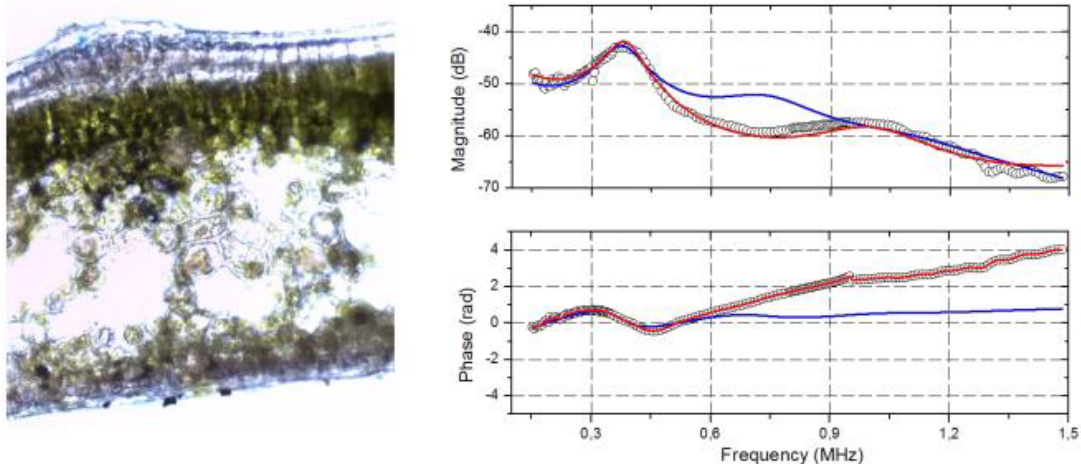


**Figure 22.:** Cross-section (*left*) and transmission coefficient spectra (*right*) of an *Abelia edward goucher* leaf. Dots are experimental results (air-coupled ultrasound spectroscopy), blue line represents the one-layer fitting and red line the two-layer fitting. (Fariñas and Álvarez-Arenas, 2015)

However, due to the layered structure, harmonic distortion takes place and the second resonance peak is at a higher frequency. The two-layer model fits well to this peak (red line fig. 22). By contrast, in *Ligustrum* leaves, palisade parenchyma and spongy mesophyll are not so different, and the measured second resonance peak is the double the first one (see fig. 18).

Thus, there is a relationship between the distortion of the frequency pattern measured in respect

to the theoretical one-layer model and how acoustically different are the constituent layers of the leaf. Furthermore, the resonances are very sensitive to leaf microstructure. Measuring different leaves per species, a wide range of microstructures is considered and the obtained values have high standard deviations. From the ultrasonic measurements the leaves acoustic impedance, attenuation coefficient, surface density and thickness-velocity ratio are obtained (tab. 2). (Fariñas and Álvarez-Arenas, 2015)

**Table 2.:** Acoustic properties of measured plant species. Mean and standard deviation of more than 10 different measurements per species. The first layer refers to upper epidermis and palisade parenchyma, the second layer to spongy mesophyll and lower epidermis. (Fariñas and Álvarez-Arenas, 2015)

Species	Layer	Impedance [MRayl]	Surface density [kg/m <sup>2</sup> ]	Attenuation [Np/m]	Velocity/thickness [MHz]
<i>Abelia</i>	1	0.864 ± 0.130	0.196 ± 0.015	28.8 ± 27.1	4.21 ± 0.732
	2	0.119 ± 0.017	0.088 ± 0.012	18.7 ± 34	1.351 ± 0.047
<i>Li-guistrum</i>	1	0.419 ± 0.081	0.525 ± 0.198	12.8 ± 7.3	1.403 ± 0.654
	2	0.239 ± 0.077	0.156 ± 0.061	12.2 ± 2.6	1.119 ± 0.139

### Three-layer model

Other than the two-layer model, some information of the sample needs to be known or measured independently.

For the three-layered medium approach, the first three thickness resonances are analyzed. The analysis works as for the one-layer model, but for the transmission coefficient there is no analytical solution (as in equation 35 for instance). Instead, the so obtained data from the one-layer model is used as initial guess. A layered structure is assumed, where initially all layers are equal (with the properties from the one-layer model). Then some parameters of the multi-layered model are allowed to be changed in the Gradient Descent algorithm (densities, ultrasound velocity and attenuation of each layer) in search of the best layer properties to fit the calculated with the measured spectra. But it is necessary to know how many layers are necessary to produce a reasonable acoustical representation of the leaf, the thickness of each layer and the overall density in order to reduce the number of parameters and extract meaningful information. Results are shown in figure 23.

(Fariñas and Álvarez-Arenas, 2014)

### Four-layer model

With a four-layered model, each of the four layers of a leaf can be represented. However, detailed information about the layers is needed. To show the effects of a multi-layered structure on the transmission coefficient spectrum, the one-layer spectrum for a *Prunus laurocerasus* leaf is calculated, based on typical values for the parameters  $t$ ,  $\rho$ ,  $v$  and  $\alpha$ . The same parameters are estimated for each of the four different layers upper and lower epidermis, pallisade parenchym and spongy mesophyll and the four-layer transmission coefficient spectrum is calculated. Compared to the one-layer one, three main differences appear: The resonance frequency shifts, the insertion loss is larger and the regular resonance pattern is distorted: the periodicity is lost and the pattern completely disappears at high frequencies (fig. 24).

(Álvarez-Arenas et al., 2009a)

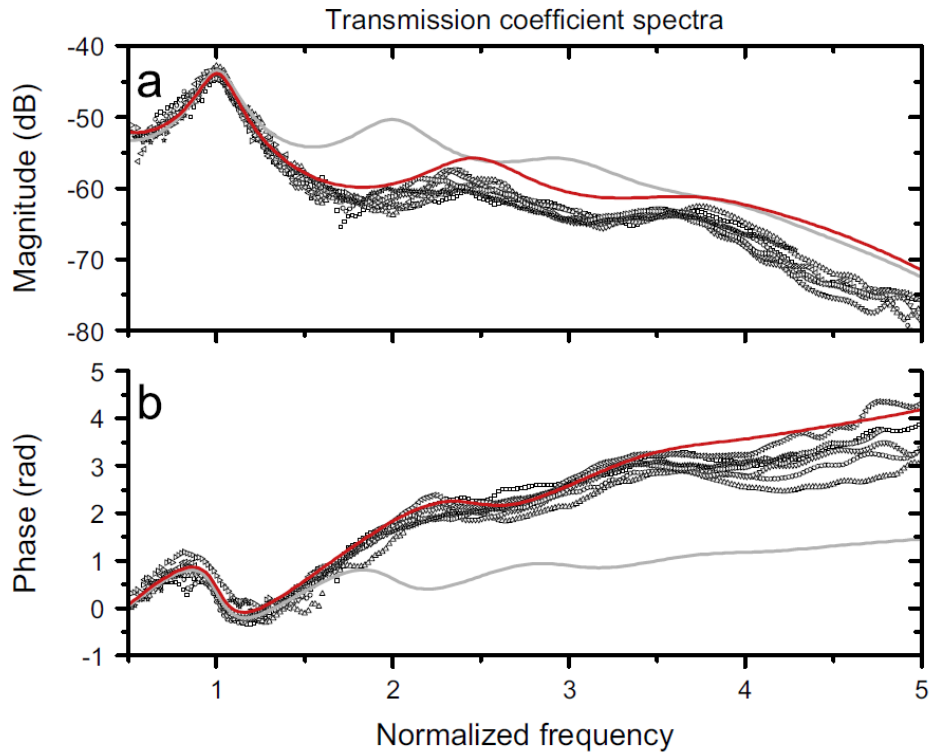


**Figure 23.:** Magnitude and phase spectra vs. normalized frequency (1 = first resonance) in seven different thickness points of a leaf of *Phormium tenax*. Dots are experimental data, solid grey line represents the one-layer model and solid red line the three-layer model. (Fariñas and Álvarez-Arenas, 2014)

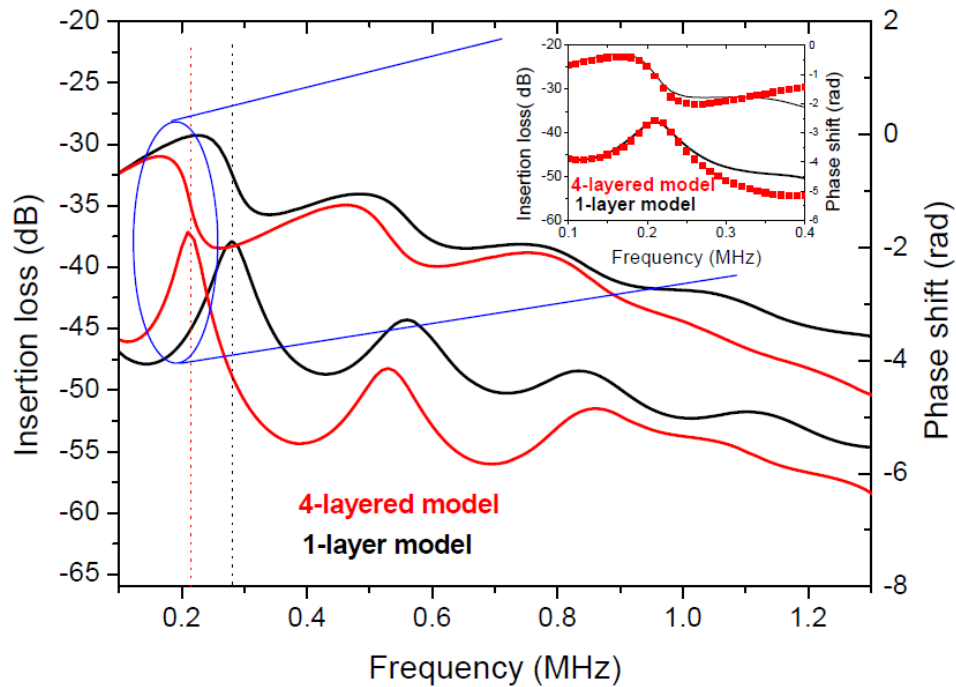


**Figure 24.:** Magnitude and phase spectra calculated for a typical *Prunus* leaf with a one-layer model (black line) and with esteemed values for the four different layers (red line). For details concerning the inset, please see Álvarez-Arenas et al. (2009a)

## 2.4. Biological relevance

As mentioned above, ultrasonic techniques have been applied to plant leaves. (Air-coupled) ultrasound spectroscopy offers the possibility to study plant leaves in a non-contact and non-invasive way. A huge advantage is that no water immersion is needed, therefore also variations of water content or turgor pressure can be studied. The technique can also be applied to attached, naturally transpiring leaves (fig. 25). A continuous monitoring in real time is possible. (Fariñas et al., 2014). Both ultrasonic and mechanical properties of the leaves can be obtained from the measurements (for details and examples see section Ultrasonic Spectroscopy). Other than the sample's thickness and density, its elastic constant in thickness direction can also be derived. Moreover ultrasound technique has the potential to sense the variations in leaf properties caused by the plant's response to different environmental stimuli, especially concerning the leaf's water content. Therefore ultrasonic spectroscopy provides a huge potential for applications in physiological studies on plants as well as in the continuous monitoring of plant water status as required in agriculture. (Sancho-Knapik et al., 2011)



**Figure 25.:** Air-coupled transducers attached to a *Vitis vinifera* plant. (Fariñas et al., 2014)

There are basic mechanisms that link physiological and ultrasonic properties of the leaf. At the core of this link is the hierarchical multiscale organization of biological materials. The plant is able to structurally respond with high efficiency on every hierarchical level. A variation in the water content causes different cell deformability that is one of the key links between physiological properties and the properties of the spectrum of leaf thickness resonances (fig. 26). (Fariñas et al., 2014)

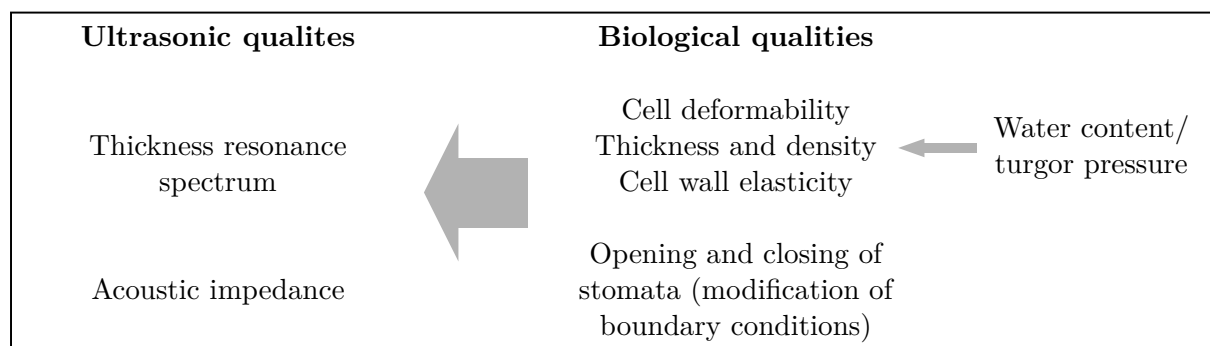


**Figure 26.:** Ultrasonic and biological properties of plant leaves. (Derived from Fariñas et al. (2014))

Ultrasound measurements used to obtain the leaf parameters thickness, density, velocity and attenuation coefficient of different species suggest a close relationship between ultrasonic parameters and leaf development stage, environmental conditions or type (evergreen or deciduous), that can be attributed to a variation in leaf morphology and composition (distribution of different layers, presence of resinous substances). (Álvarez-Arenas et al., 2009a,b)

Moreover, the ultrasonic qualities of leaves seem to be very sensitiv towards variations in the leaf's water status and water content. Álvarez-Arenas et al. (2009a,b) and Álvarez-Arenas (2010) investigated the drying process of leaves of different species, left to dry at ambient conditions. They found a decrease in resonance frequency (fig. 28), velocity and thickness during the drying process (notice that no thickness reduction has been observed in Álvarez-Arenas et al. (2009a)). Attenuation on the other hand increased.

The velocity decrease can be explained by the increase of compressibility of the cells due to a loss of water and thus decrease of turgor pressure and rigidity. A decreased velocity leads to lower resonance frequencies (eq. 33). Attenuation however is higher in compressible media. As a consequence of water loss, thickness reduces but density remains constant because the loss of water is compensated by volume decrease.

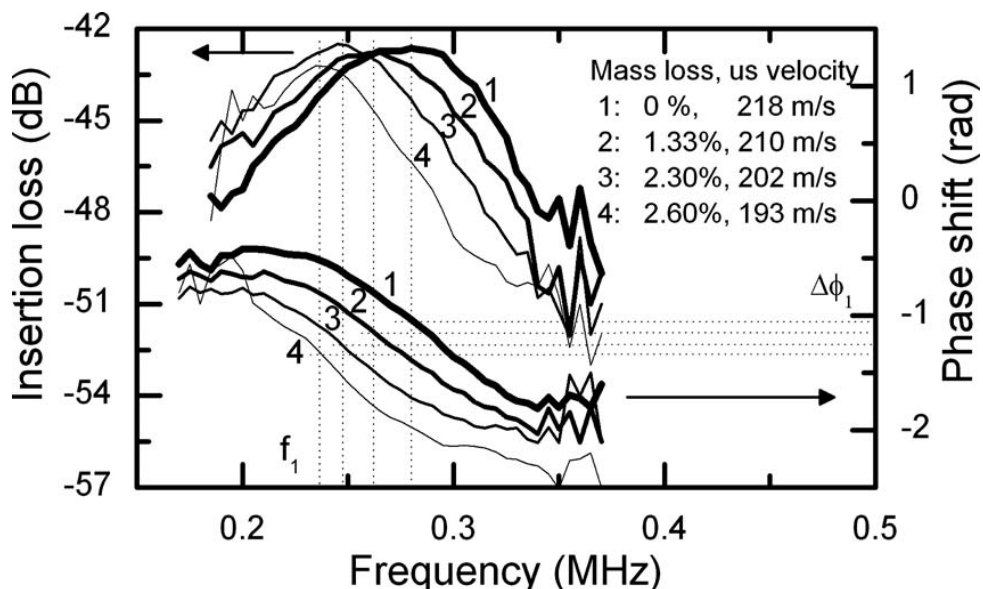


**Figure 27.:** Insertion loss and phase shift vs. frequency of a *Prunus laurocerasus* leaf as water content decreases (from 1 to 4). A shift of the resonance frequency towards lower values as the leaf is left to dry can be observed. (Álvarez-Arenas et al., 2009b)

To gain a better understanding for this strong relationship found between the leaf's relative water content (RWC) and (standardized) frequency of thickness resonance, Sancho-Knapik et al. (2010) studied the structural changes occurring during leaf dehydration further. To reveal more about the link between the leaf's physiology and its ultrasonic properties, *Quercus muehlenbergii* leaves were investigated in terms of ultrasound measurements, P-V analysis, leaf thickness and leaf structure. They found a sigmoid relationship between the RWC and the standardized resonance frequency in *Quercus muehlenbergii* leaves (fig. 27). The turgor loss point was obtained, that separates two different phases of the performance of resonance frequency as a function of RWC variations. In the first phase with high RWC, the turgor pressure decreases and a reduction in the macroscopic effective elastic constant ( $c_{33}$ ) is the main factor explaining the decrease in resonance frequency. In the second phase the variations of ultrasonic properties might be explained by physical changes found in the mesophyll.

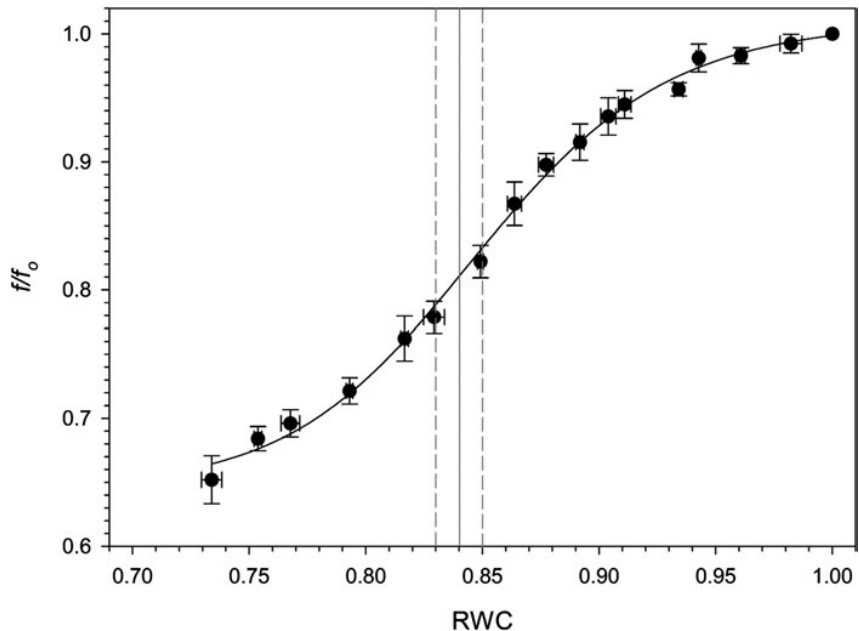


**Figure 28.:** Relationship between the relative water content (RWC) and the standardized frequency ( $f/f_0$ ) for *Quercus muehlenbergii*. The solid line indicates the estimated relative water content at the turgor loss point, the dashed line the standard error of this estimation. (Sancho-Knapik et al., 2011)

Sancho-Knapik et al. (2012) focused on the study of the elastic constant in thickness direction ( $c_{33}$ ) obtained from the thickness resonances and found that it provides a very good indicator of the leaf status.  $c_{33}$  decreases when the leaves lose water, that can be attributed to the loss of tension in the cell membranes and the deformation of the cell structure. The observed variations in  $c_{33}$  with water content are even larger than the ones observed in the standardized resonance frequency and can therefore provide a good procedure to determine RWC of leaves.

Recently, Fariñas et al. (2014) investigated the possibility of using ultrasound technique to sense variations in leaf properties caused by the plants response to different environmental stimuli. Different species with different types of leaves were considered: *Hibiscus rosa-sinensis*, *Vitis vinifera*, *Draceana marginata* and *Epipremnum aureum* (for *E. aureum* one plant grown without exposure to direct sunlight, one plant grown under direct sunlight). In the ultrasonic response, the variations in thickness resonance frequency ( $f_{res}$ ) are taken into account. Three cases for environmental stimuli were investigated:

**Sudden change in light intensity** After 1h of direct sunlight exposure, the light intensity was drastically reduced.  $f_{res}$  increases in the dark, until a maximum value is reached. This can be explained as follows: Due to the stomata closure (reduction in transpiration) and increased leaf water potential, the leaf RWC and turgor pressure increase in darkness. This shifts the resonance frequency towards higher values, because ultrasound velocity is increased in the stiffened tissues caused by the turgor pressure increase.

**Sudden watering** The plants were not watered for several days and then amply watered.  $f_{res}$  increases when watered, until a maximum value is reached. There is a clear difference in the variation of the frequency shift between the species.

This can be explained as follows: First, the resonance frequency shift to higher frequencies is due to the increase in RWC and turgor pressure (as explained above) and determined by the leaves

properties (how much does the cell wall tautness can change with RWC; cell-wall elasticity). Second, the kinetic of the process are determined by the velocity of water transport from soil to leaf (vascular system).

Noticeable is also a comparison between the frequency shift at drought ( $t = 0$ , before watering) and the frequency shift measured at the turgor loss point. For *D. marginata*, the frequency shift is considerable smaller than at the TLP, meaning water loss is limited well before the turgor loss point. For *H. rosa-sinensis* and *V. vinifera*, both magnitudes are similar, meaning that their RWC was reduced near to the TLP.

**Diurnal cycle of solar radiation** The plants were measured for 3-4 days.  $f_{res}$  with the time of the day follows the variations in light intensity (fig. 29). The sensitivity of the resonance frequency to light intensity differs between species, but the minimum value of  $f_{res}$  is always at the maximum of light intensity. The variations of  $f_{res}$  over the time in the different species are similar to those measured after a sudden change in light intensity, so the main factor affecting the thickness resonances seems to be light intensity (leading to a change in the turgor pressure). The kinetics of the frequency shift and the presence of saturation levels seems to depend on the mechanisms these plants use to adapt to the sunlight intensity (differences in species and environmental conditions under which the plants have grown).

(Fariñas et al., 2014)

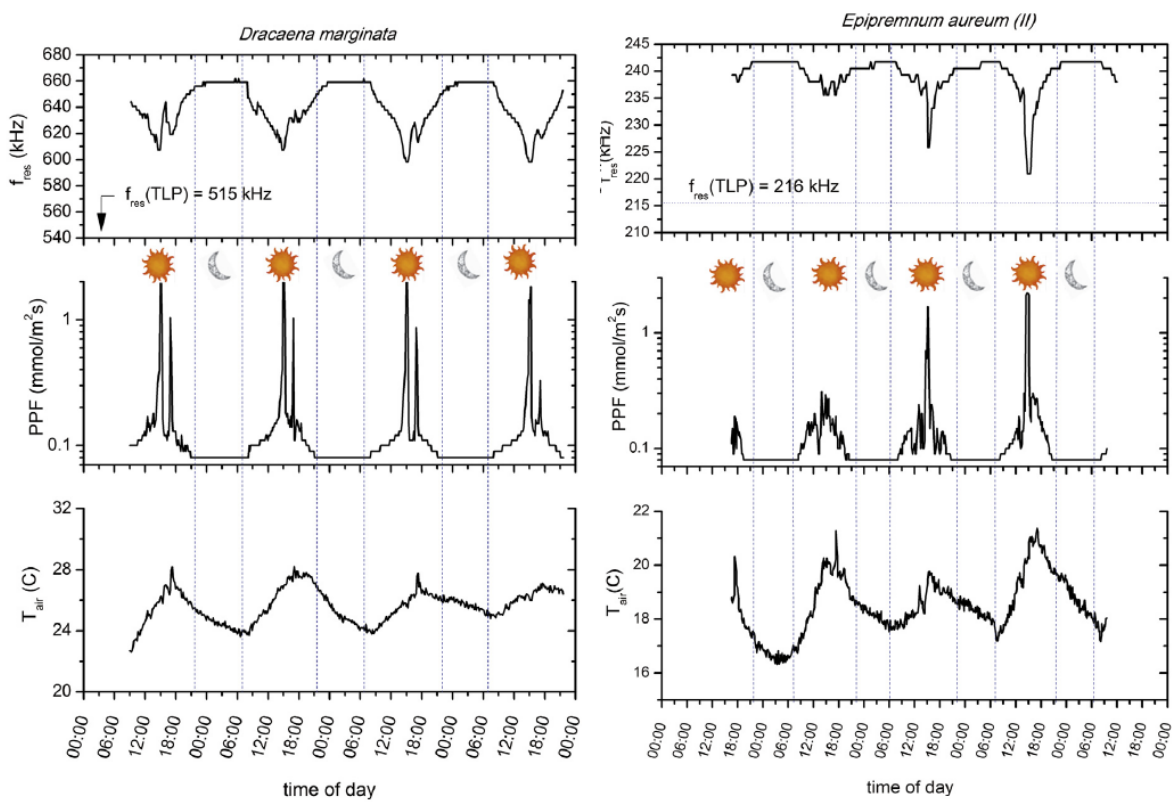


**Figure 29.:** Evolution of the thickness resonant frequency of a *Dracaena marginata* leaf (left) and a *Epipremnum aureum* leaf (right) over 3.5 days.  $f_{res}$  (TLP) indicates the resonance frequency at turgor loss point (measured separately). Photosynthetic photon flux (PPF) and ambient temperature measurements are also shown. (Fariñas et al., 2014)

## 3. Experimental work

### 3.1. Methods

#### 3.1.1. Experimental setup

The ultrasound spectroscopy setup consists of a cylindrical ultrasonic transducer (1 MHz,  $\phi=23$  mm) and a hydrophone (1 mm needle probe attached to a preamplifier, supplied with power via a DC Coupler) (both Precision Acoustics, Dorchester, UK). Transmitter transducer and hydrophone are facing each other with the sample in between. The setup is immersed in water and hydrophone and transmitter transducer are connected to a pulser/receiver (Pulser/Receiver DPR 300, JSR Ultrasonics, Imaginant, Pittsford, USA; 475 V and 35 MHz bandwidth) and an oscilloscope (Infinii Vision DSO-X 3024T digital storage oscilloscope, Keysight Technologies, Wokingham, UK) as shown in fig. 46.

Transducer, hydrophone and sample are attached by holders to slides on a scaffold. Distances (x-axis) and angles are adjustable, as well as height (y-axis) for the sample holder (see fig. 47). The scaffold can be moved over a fish tank containing distilled water for measurements and be removed for storing and sample changes. Samples are held by frames in different sizes. Detailed information on how to use the setup can be found in the appendix A.

A risk assessment has been carried out (see appendix A).

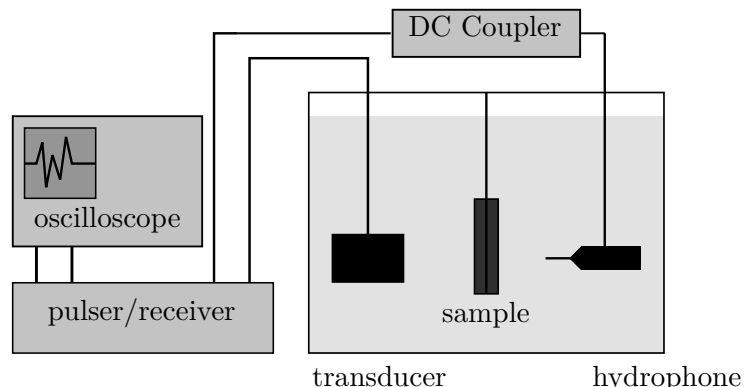


**Figure 30.:** Experimental Setup. Transducer and hydrophone are immersed in a fish tank filled with distilled water. The pulser/receiver drives the transducer to launch a signal through the sample to the hydrophone, from where it is then transferred back to the pulser/receiver again for amplification and filtering and finally the signal is displayed on the oscilloscope.

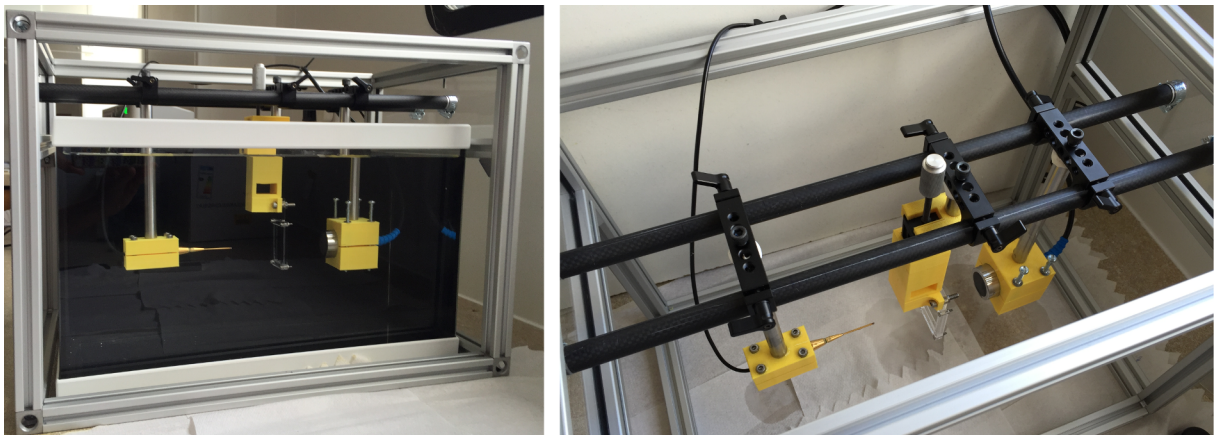


**Figure 31.:** Experimental Setup. The actual measurement situation is shown (*Left*) as well as the scaffold removed from the fish tank (*right*). Slides to adjust distances as well as positioner for the adjustment of sample hight are visible.

To obtain a picture of the signals, the following settings proved useful; if not otherwise indicated, these are the ones used for the results discussed here.

**Pulser/receiver:** Pulse repetition frequency (PRF) 1 (100 Hz), pulse amplitude 7 (164.0625 V), pulse energy 1 with Z high, damping 1 ( $331 \Omega$ ), relative gain 38, HP Filter out and LP Filter at 35 MHz.

**Oscilloscope:** avaraging 200 times; BW Limit off

Several measurements to characterize the setup have been carried out and are discussed below. The ultimate aim of the measurement is to obtain magnitude and phase spectrum with thickness resonances, appearing when the frequency is such that the reflections inside the sample are constructive and therefore transmission maximal. A glass microscope slide of 1 mm thickness was used as a sample. With the speed of sound in glass of 4540 m/s (NDT), the time needed for the signal to travel through the sample is  $2.2026e-07 \text{ s} \approx 0.22e-06 \text{ s}$ . To acquire the data from the oscilloscope, a time resolution of 1  $\mu\text{s}/\text{div}$  was chosen, the data covered then a time window of  $9.975e-06 \text{ s}$ . Multiple reverberations from within the plate are thus largely covered by this setting.

The expected first resonance for glass is at 2.27 MHz (eq. 30). Carrying out the analysis, the frequency spectrum is therefore reduced to a corresponding range.

### 3.1.2. Data analysis

To obtain the magnitude and phase spectrum, the following analysis was carried out in MATLAB R2014b to obtain the sample's frequency and phase spectrum via the fast fourier transformation (FFT), in this example for the measurement number hydri1.

```
%Import data
seconds=hydri1 (:,1);
volt=hydri1 (:,2);
v=volt (2:1998); %remove first and last row(s) (NaN sometimes)
s=seconds (2:1998);
%Plot original signal
figure
plot(s, v)
title( 'Measured_Signal')
xlabel( 'time_in_seconds')
ylabel( 'Volts')
```

```

%calculate FFT
N=4096; %FFT length ;
X=fft (v,N);
amplitudeV=abs(X(1:200));
%sampling frequency
time=s(1997)-s(1); %time covered by signal
fs=1997/time; %1997 points taken in that time
%frequency bin , frequency resolution of FFT
fd=fs/N;
sampleIndex=0:(N-1);
%frequency scale
f=sampleIndex*fd;

figure
plot(f,abs(X))
title('FFT')
xlabel('frequency -Hz')
ylabel('Volts')

p = unwrap(angle(X));
figure
plot(f,p)
title('phase')
xlabel('frequency -Hz')
ylabel('rad')

phase=p(1:200); %take only first part of frequency range
freq=f(1:200);
magnitude=20*log(abs(X(1:200))); %decibel

figure
subplot(1,2,1)
plot(freq,magnitude)
title('magnitude')
xlabel('frequency -Hz')
ylabel('phase')

subplot(1,2,2)
plot(freq,phase)
title('phase')
xlabel('frequency -Hz')
ylabel('phase')

%save as .dat file
save phase_hydrdi1.dat phase -ascii
save amplitude_hydrdi1.dat magnitude -ascii
save amplV_hydrdi1.dat amplitudeV -ascii
save freq_hydrdi1.dat freq -ascii

```

To work out the material properties from the spectrum, the incident pulse (without sample) and the transmitted pulse (with sample) are compared by taking the difference of the transmitted phase spectrum minus the incident and the transmitted magnitude spectrum ([dB]) minus the incident. The analysis was carried out in MATLAB R2014b as follows for the example measurement tta4 and the result introduced into the python code provided by the us biomat group and run in Enthought Canopy (Version 1.7.2.) to obtain the material properties.

```
%Import data as numeric matrix
%take difference
phase=phasetta4-phasetta4i;
amplitude=amplitudetta4-amplitudetta4i;
freq=freq;
f=freq';

figure
subplot(2,1,1)
plot(f, amplitude)
title('Magnitude-spectrum')
xlabel('Frequency-Hz')
ylabel('db')
subplot(2,1,2)
plot(f, phase)
title('Phase-spectrum')
xlabel('Frequency-Hz')
ylabel('rad')

%save results in table, specify length of signal to be taken
spectrumtta4=table(f(1:100), amplitude(1:100), phase(1:100));
writetable(spectrumtta4, 'spectrumtta4.dat', 'Delimiter', ',', 'writevariableNames', false);
```

## 3.2. Results and discussion

### 3.2.1. Characterization of setup

To gain a better understanding on how the setup works, different parameters were investigated to enable an annotation of the observed picture of pulses and echoes.

#### Distance between transducer and receiver

The sample holder was put approximately in the middle between transducer and hydrophone. Three positions for transducer and hydrophone were taken: maximum distanced in the tank, then an intermediate distance and finally very near to the sample. Every stage was measured with and without a sample (glass slide) mounted to the holder.

The expected outcome was to observe a change in the position of the received signal in time domain but not in frequency domain. Due to the attenuation in water a decrease in amplitude should be observed with increasing distance.

The result is shown in fig. 32. Due to the distance change, the first received pulse (traveling the direct distance), as opposed to the sent pulse can be clearly identified moving nearer to the sent pulse as distance shortens and thus time of flight reduces. Also, various echoes can be seen that arrive later. A more detailed analysis in time and frequency domain of the first pulse (fig. 33 and 34) show that as expected in terms of frequency content there is no big difference

between the measurements taken at different distances, although an increase in amplitude can be observed with decreased distance. Transferring the amplitude into the logarithmic unit decibel, the apparent difference becomes much smaller.

For the sake of completeness, the results for the same measurements with a glass slide sample mounted to the setup can be seen in the appendix B.

### **Introduction of a sample**

Measurements were taken (for a fixed distance) with and without a glass sample mounted to the sample holder (averaging of signal was less than the otherwise used 200 times). If one compares the measurements with and without sample in between, the following is noticeable (fig. 35): With the sample, the amplitude of the first received pulse is smaller. This is due to the fact that only a part of the wave is transmitted through the sample and the rest reflected back, whereas without the sample no such barrier is present. Secondly, the pulse that travels through the sample is quicker than the one without sample. This is an expected outcome as the speed of sound is faster in glass (4540 m/s, NDT) than in water (1482.3 m/s, McClements and Gunasekaran (1997)).

### **Position of sample**

Transducer and hydrophone were positioned at maximum distance in the tank. Three different positions of the sample holder with and without sample (glass slide) were measured: Sample holder near hydrophone, sample holder in the middle between hydrophone and transducer and sample holder near transducer. To get a better picture of the signal, the energy setting on the pulse/receiver was changed from 1 to 3 (Z high).

The expected outcome was that the change of the position of the sample does not effect the received first pulse, neither in frequency nor in time domain as the overall distance and thus time of flight stays the same. Moreover also the amplitude of the signal should stay the same as the overall attenuation does not change, only the point at which the signal is split into reflected and transmitted part. Additionally the comparison of measurements should allow a more thorough understanding of the pulses and echoes.

The results to compare are shown in fig. 36 (to view all measurements separately, please refer to appendix C). The direct, first received pulse is clearly visible and does not change time wise with the repositioning of sample, as was expected. Moreover a pattern of smaller pulses that follow the first one can be recognized in both measurements with and without sample (between  $1 \times 10^{-4}$  and  $2 \times 10^{-4}$  s). With sample their amplitude is lower and their position does not change with the change of position of sample holder. It therefore cannot be reflections from the sample holder. It must be some other reflections that also pass through the sample if it is mounted and thus diminish in amplitude. However, it remains unclear where they come from because reflections from transducer holder or fish tank sides that would go to and fro before arriving at the hydrophone should need more time than the ones observed.

Furthermore some pulses appear only in the measurements with the sample mounted. These are probably reflections from the sample back to the transducer and only then to the hydrophone.

That could apply to the middle position (red line in fig. 36 where a pulse can be seen at ca.  $2.2 \times 10^{-4}$  s, being approximately double the first one) and to the position of sample near the transducer (yellow line), where a pulse can be seen very soon after the first one. However, the appearance of a pulse at ca.  $2.0 \times 10^{-4}$  s for the position of sample near hydrophone (blue line) remains unclear.

Fig. 37 and 38 show the results for a more detailed analysis of the first received pulse. As expected, the signal does not change in time domain with the change of sample's position. However, the amplitude of the measurement with sample near hydrophone (blue line) is lower than for the other two positions, against the expectation. This irregularity can be explained by a

### Distance shift - without sample

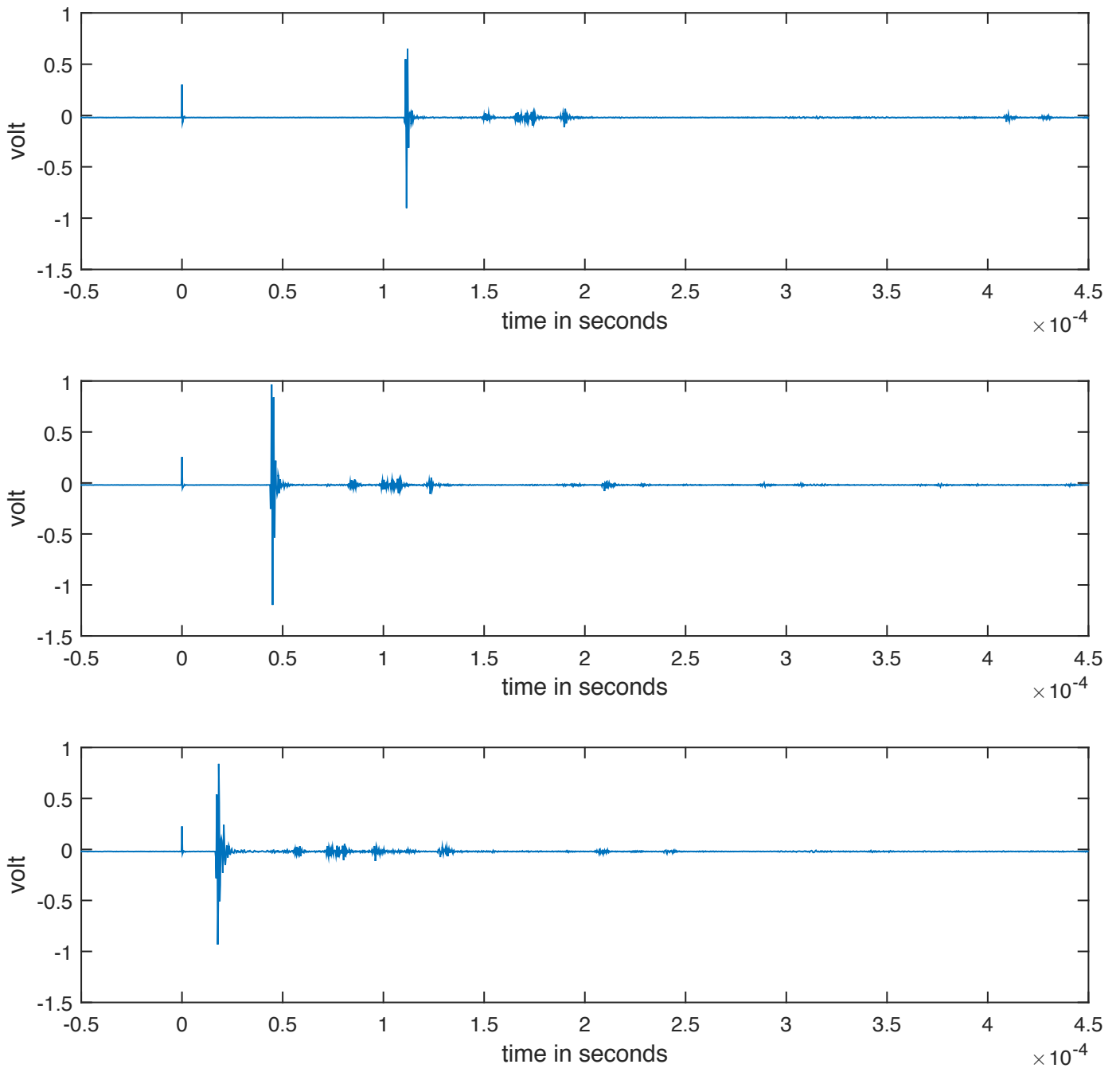


**Figure 32.:** Measured signal from transducer to hydrophone without sample in between. From *top* to *bottom* transducer and hydrophone have been moved closer together, with the empty sample holder fixed in the middle.

### Distance shift - without sample

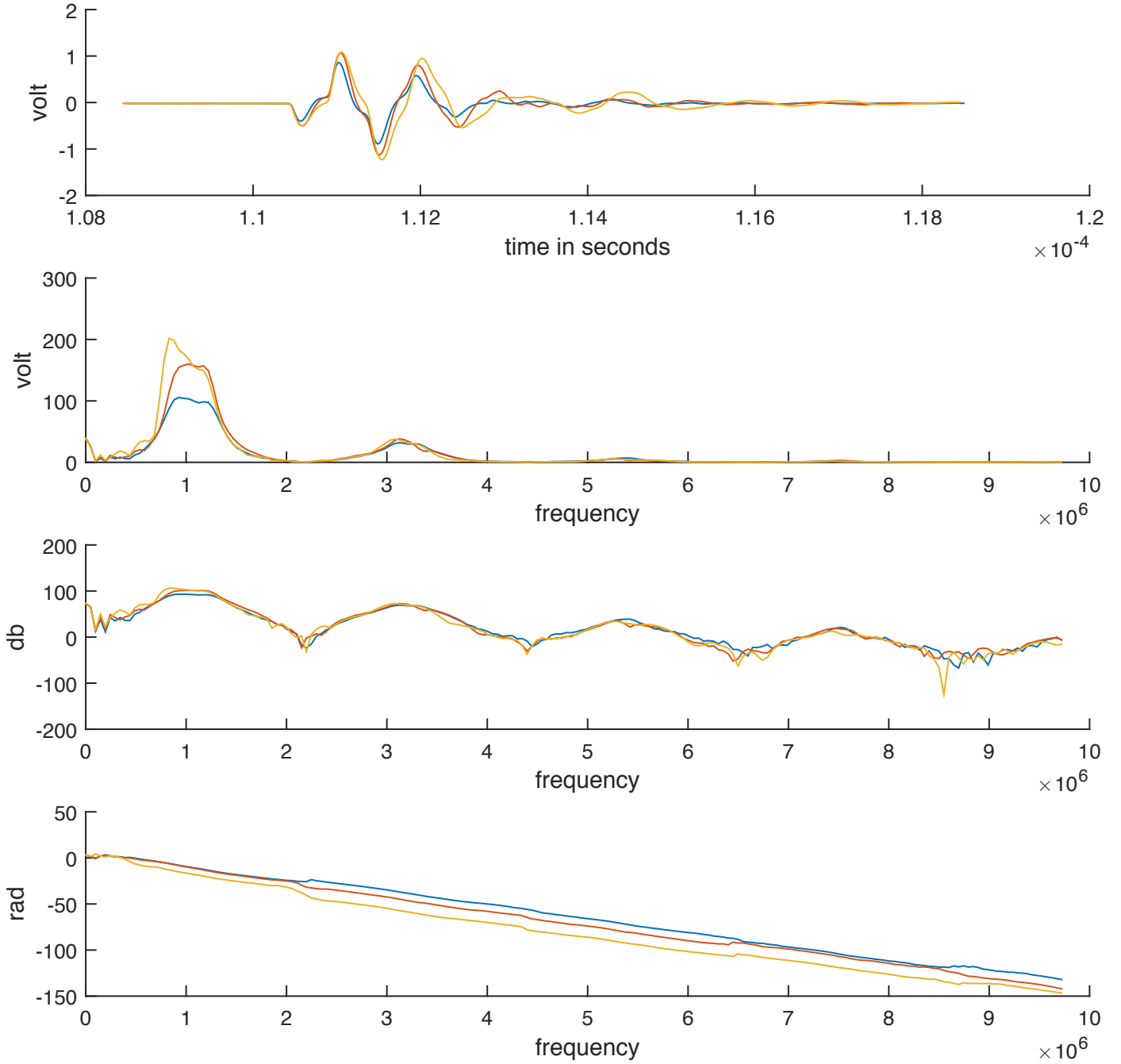


**Figure 33.:** First received pulse without the sample in between transducer and hydrophone. Comparison of a distant position (blue line), an intermediate position (red line) and a near position (yellow line) of transducer and hydrophone in the time domain (*top*), the magnitude spectrum (*middle two*) and the phase spectrum (*bottom*). To enable a comparison in time domain, the signal's position has been moved to obtain a graphical overlap.

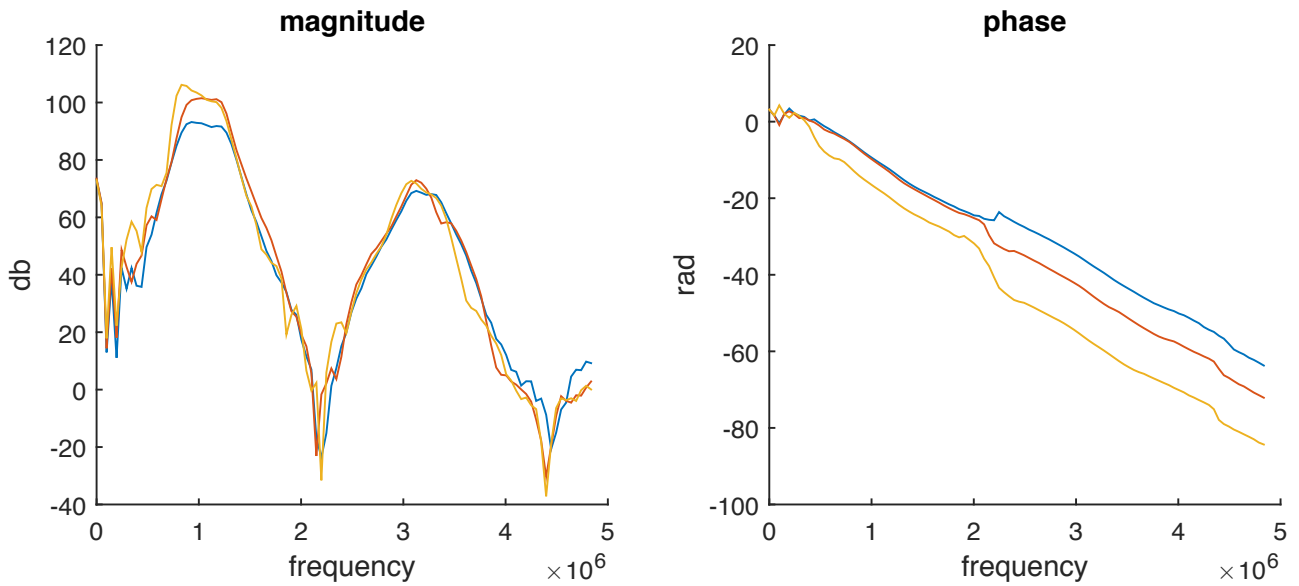


**Figure 34.:** Detail in the phase and magnitude spectrum of the first received pulse without the sample in between transducer and hydrophone. Comparison of a distant position (blue line), an intermediate position (red line) and a near position (yellow line) of transducer and hydrophone.

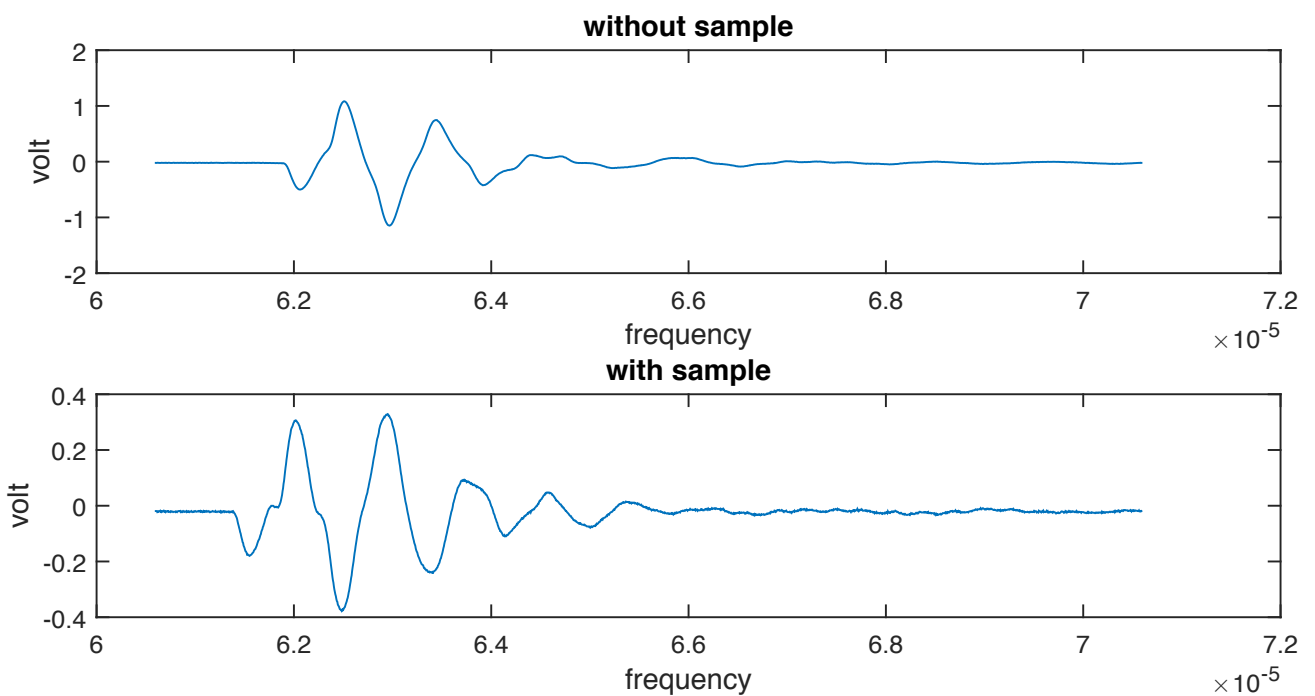


**Figure 35.:** Measured signal with and without a glass sample mounted between transducer and hydrophone.

### Position shift - without and with sample

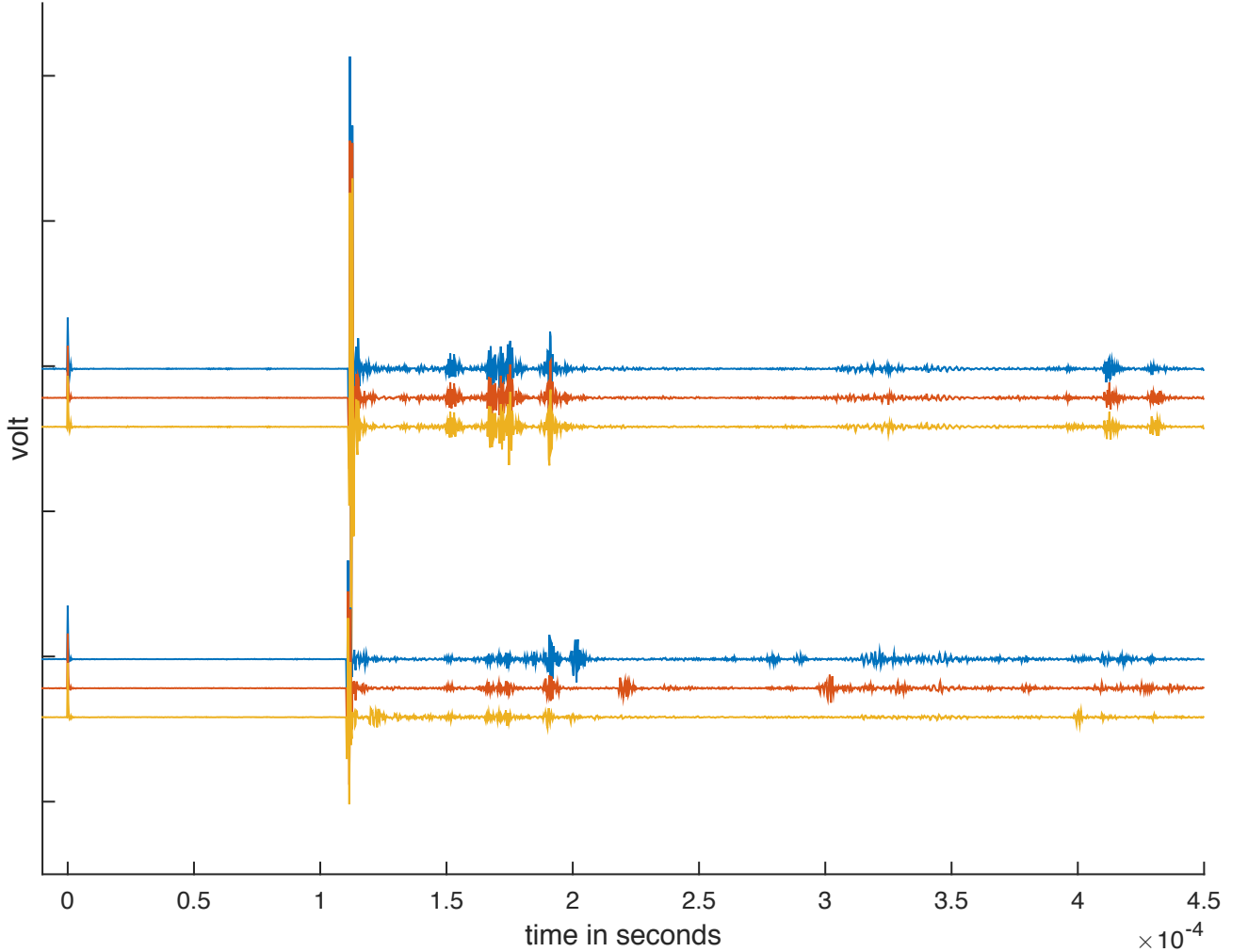


**Figure 36.:** Measured signal from transducer to hydrophone with different positions of the sample holder in between (blue line near to hydrophone, red line middle and yellow line near transducer). Measurements shown above are taken with the sample (glass slide) mounted on holder, measurements below without. To obtain a better comparison, the amplitude values in volt have been shifted.

faulty in the data acquisition that was already apparent when working with the oscilloscope: When changing the horizontal resolution, the peak value for the amplitude also decreased. This should not happen and cannot be explained so far. If one takes the maximum value measured in a lower resolution (where the entire signal can be seen, like in fig. 36), one gets a value of 0.662 V being more consistent with the other two measurements.

The results for measurements taken without the sample in between can be seen in the appendix C and show a very good agreement for the different positions.

For an analysis towards frequency domain, the distance between transducer and hydrophone as well as the position of the sample has thus no influence, as long as the pulses are still clearly visible. An other parameter is the angle at which the ultrasonic wave hits the sample and arrives at the hydrophone. The influence of how exact the desired perpendicularity needs to be adjusted has not yet been investigated though.

## Position shift - with sample

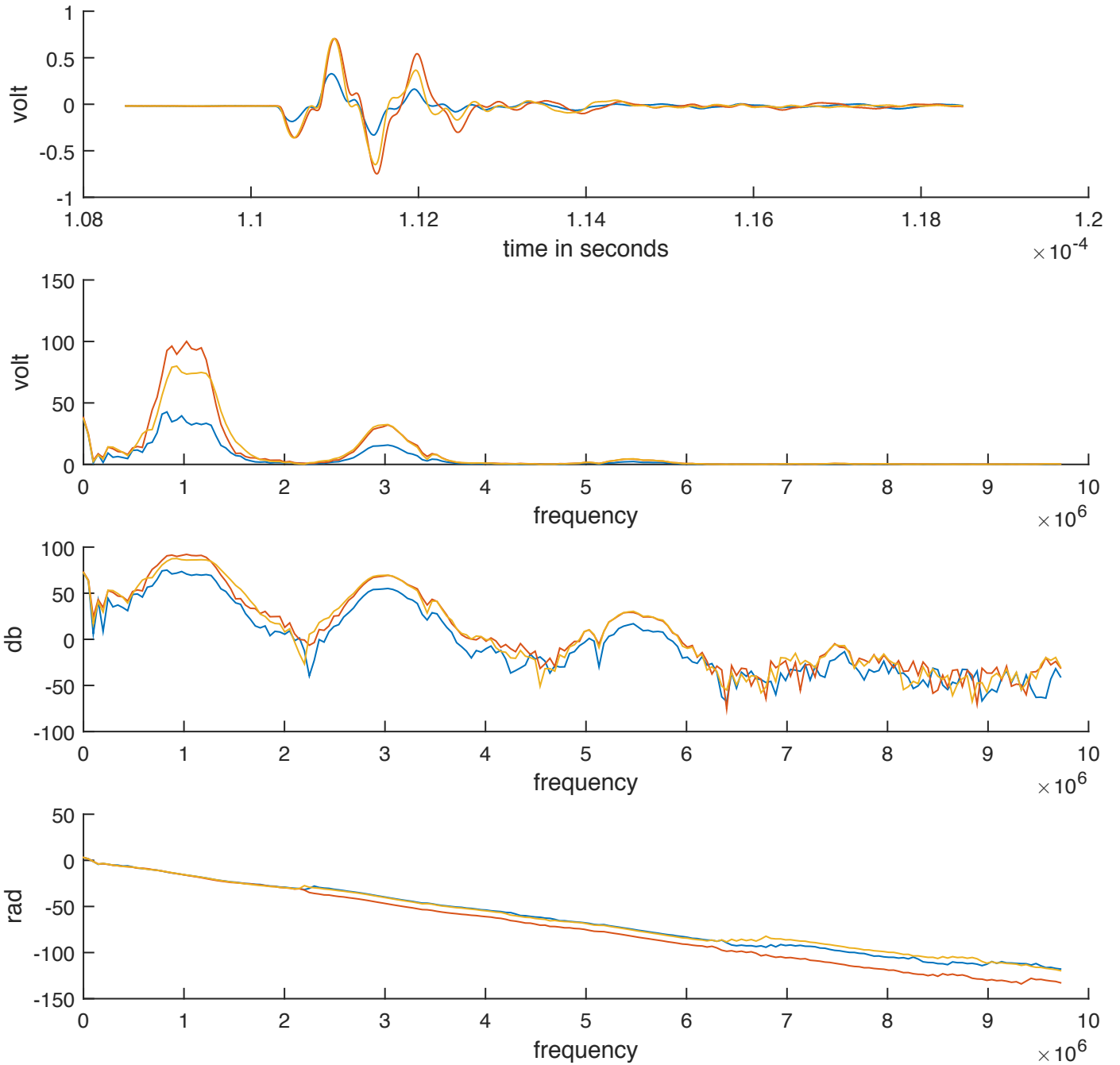


**Figure 37.:** First received pulse with the sample in between transducer and hydrophone. Comparison of the sample positioned near the hydrophone (blue line), in the middle (red line) and near the transducer (yellow line) in the time domain (*top*), the magnitude spectrum (*middle two*) and the phase spectrum (*bottom*).

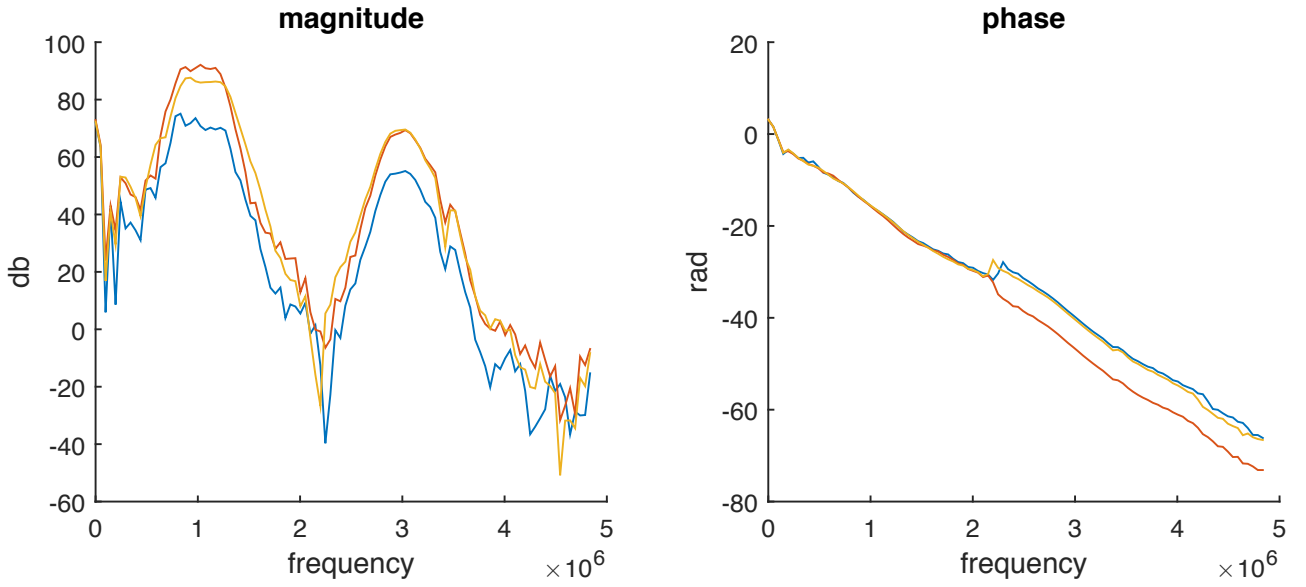


**Figure 38.:** Detail in the phase and magnitude spectrum of the first received pulse with the sample in between transducer and hydrophone. Comparison of the sample positioned near the hydrophone (blue line), in the middle (red line) and near the transducer (yellow line).

### 3.2.2. Reproducibility of measurements

Results shown so far have already given an impression on the experimental error and reproducibility of measurements. While the experiments were carried out however, a problem with the very sensible hydrophone needle occurred. It was not possible to take the needle off the preamplifier for safe storage. To make sure the sensor is still intact and not damaged while trying to take the needle off, measurements were repeatedly taken to insure consistency over time. A setup with same parameters (same settings of pulser/receiver and oscilloscope, only changes were in the number of averaging) has been put together several times over several days (measurements hydr a to f, measurement hydr c has been left out because sample was mispositioned). The distances between transducer and receiver have been newly set for every run as well as the mounting of the sample. Therefore distances may differ between the measurements, that is why a correction for the position of the signal in time domain has been introduced to obtain better comparison. Also the angle at which the sample is mounted might slightly differ between the measurements. Results for the received signal as well as the first received pulse in detail are shown in fig. 39 and fig. 40.

The reproducibility of the direct signal without the sample in between is very good. The signal measured through the sample varies considerably more between measurements. This is probably due to the fact, that the position of sample is not perfectly reproduced but may differ in angle as the sample is repeatedly mounted on the holder. Apparently the signal is very sensible to slight changes in the sample orientation. In frequency domain however, the variation is not so strong any more 41 and 42.

Analysis in frequency domain of the first pulse without sample can be found in the appendix D.

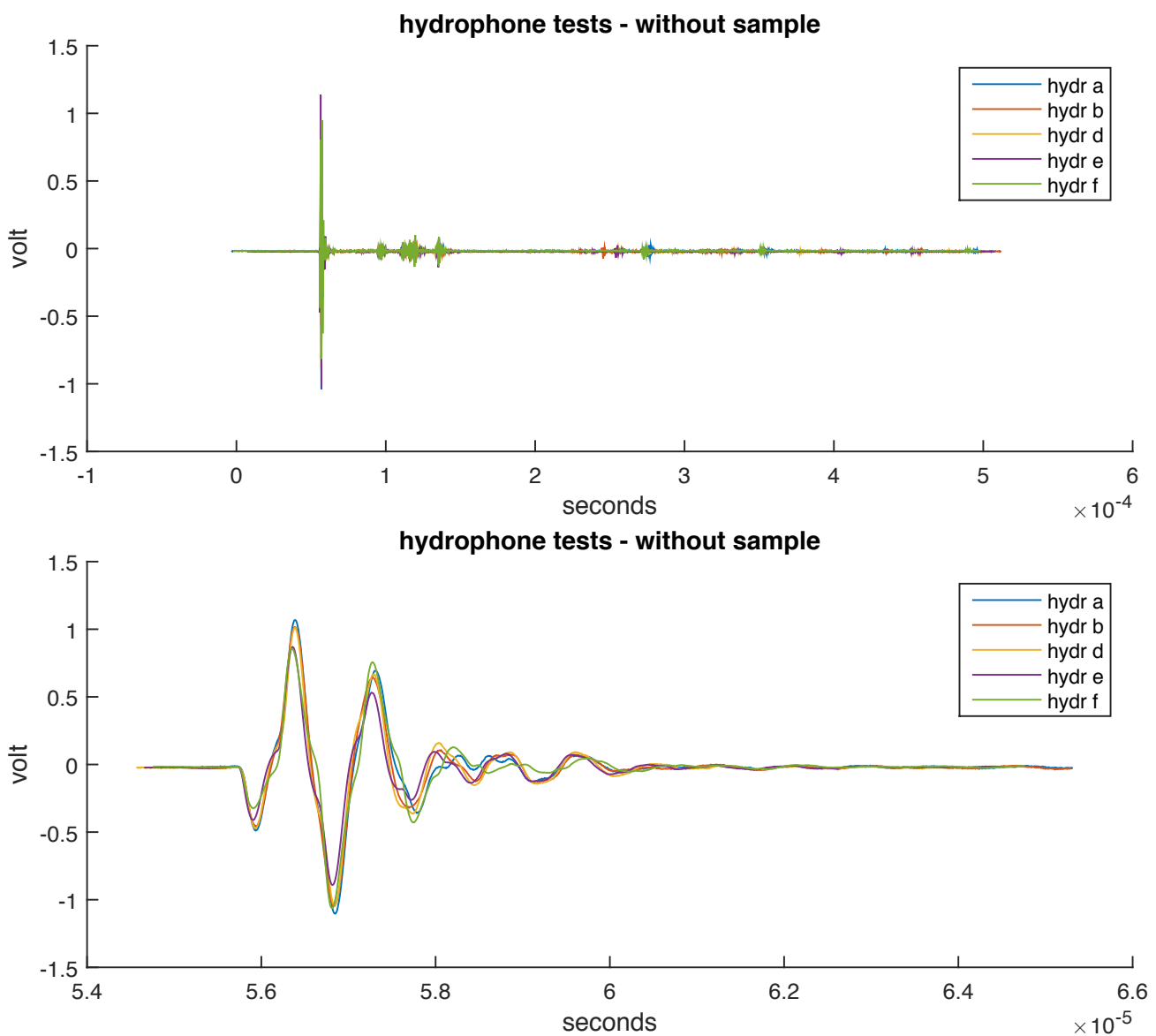


**Figure 39.:** Measured signal for repeated measurements without the sample in between transducer and hydrophone. The received signal is shown (*top*) as well as the first received pulse in detail (*bottom*). To correct for slight changes in distance that occurred while putting the setup repeatedly together, the signal has been shifted in time domain for better comparability.

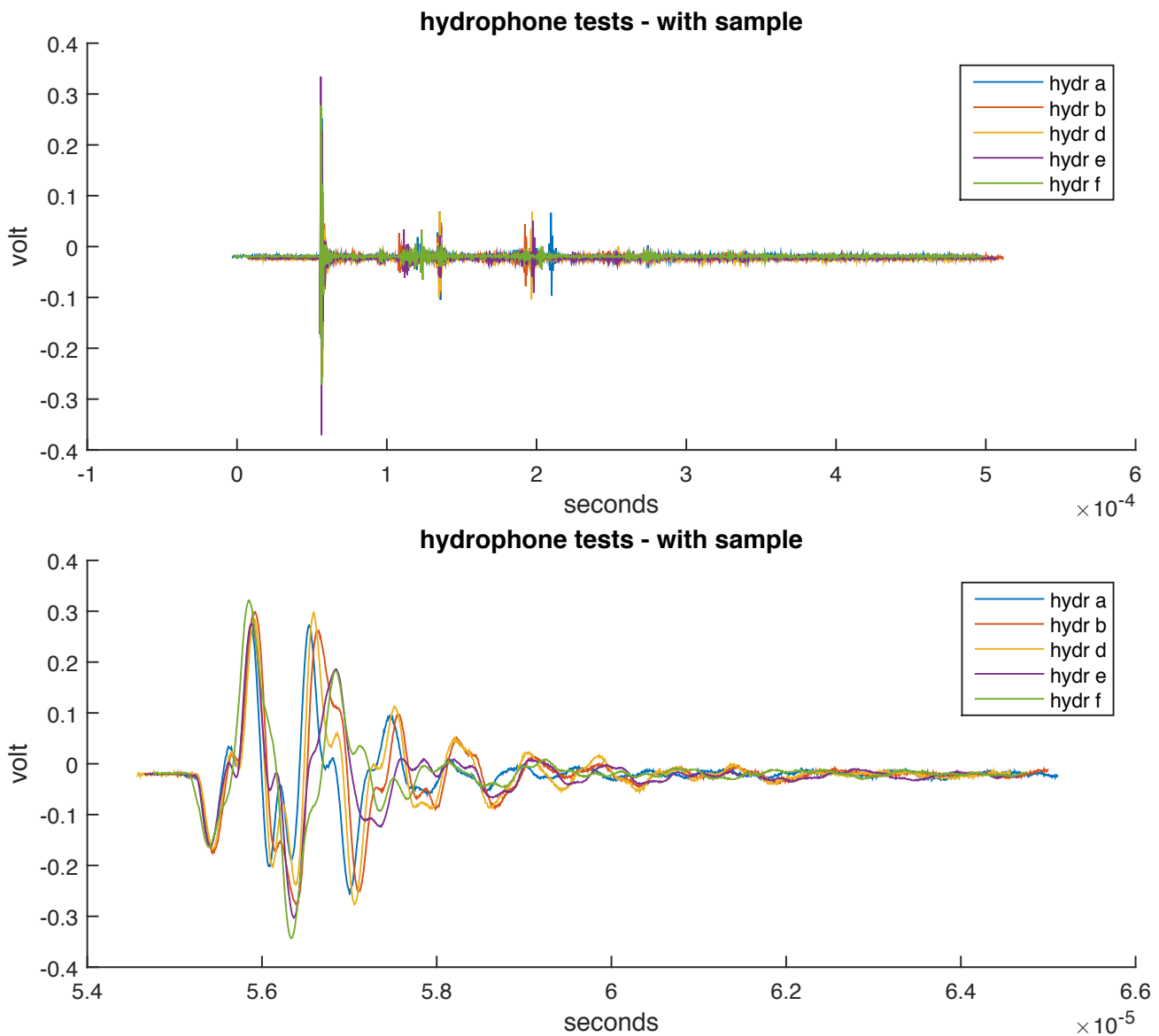


**Figure 40.:** Measured signal for repeated measurements with the sample in between transducer and hydrophone. The received signal is shown (*top*) as well as the first received pulse in detail (*bottom*). To correct for slight changes in distance that occurred while putting the setup repeatedly together, the signal has been shifted in time domain for better comparability.

## hydrophone tests - with sample

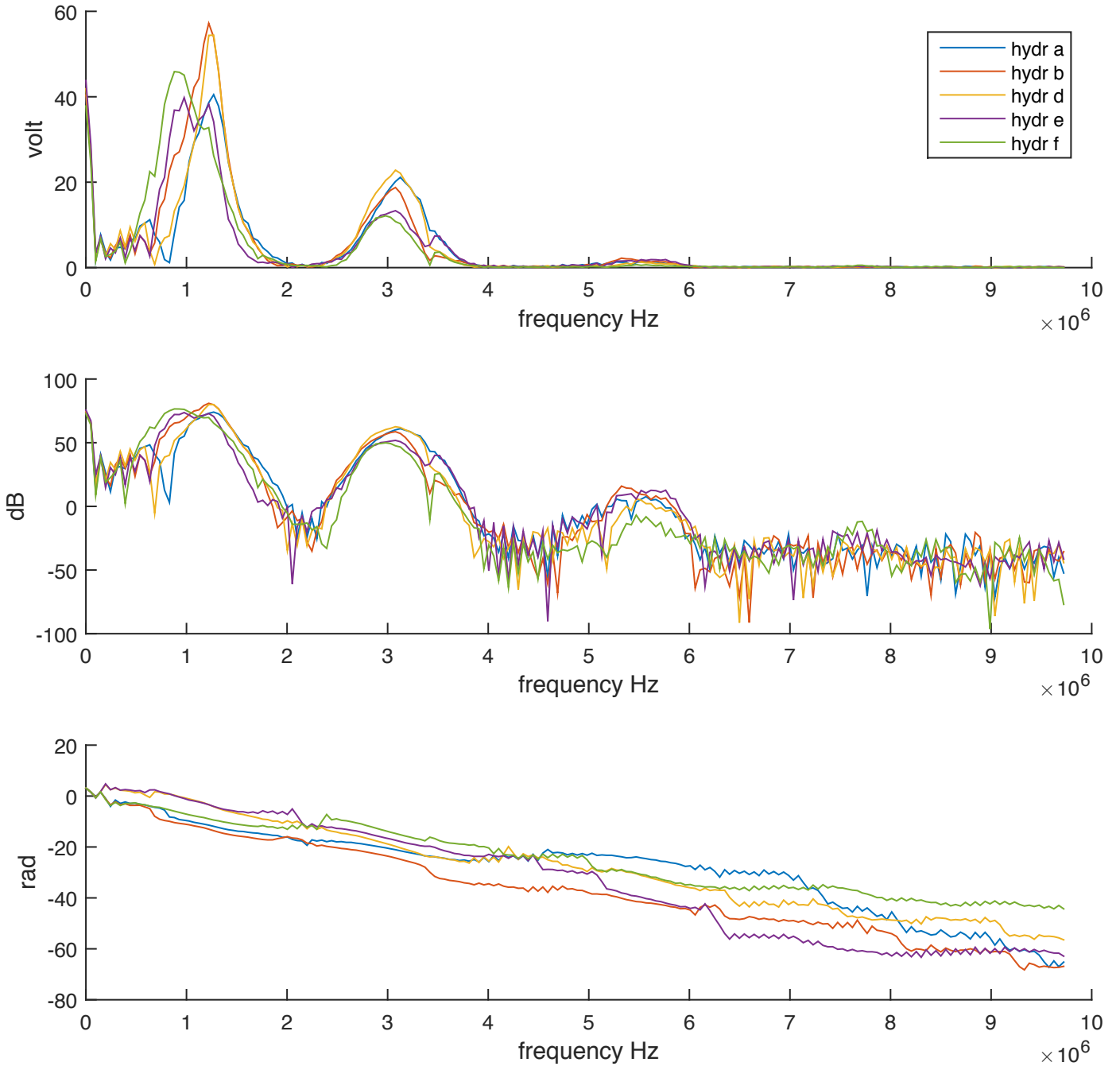


**Figure 41.:** Analysis towards frequency domain of the first received pulses through a glass sample of repeated measurements. (Pulse in time domain is shown in fig. 40)

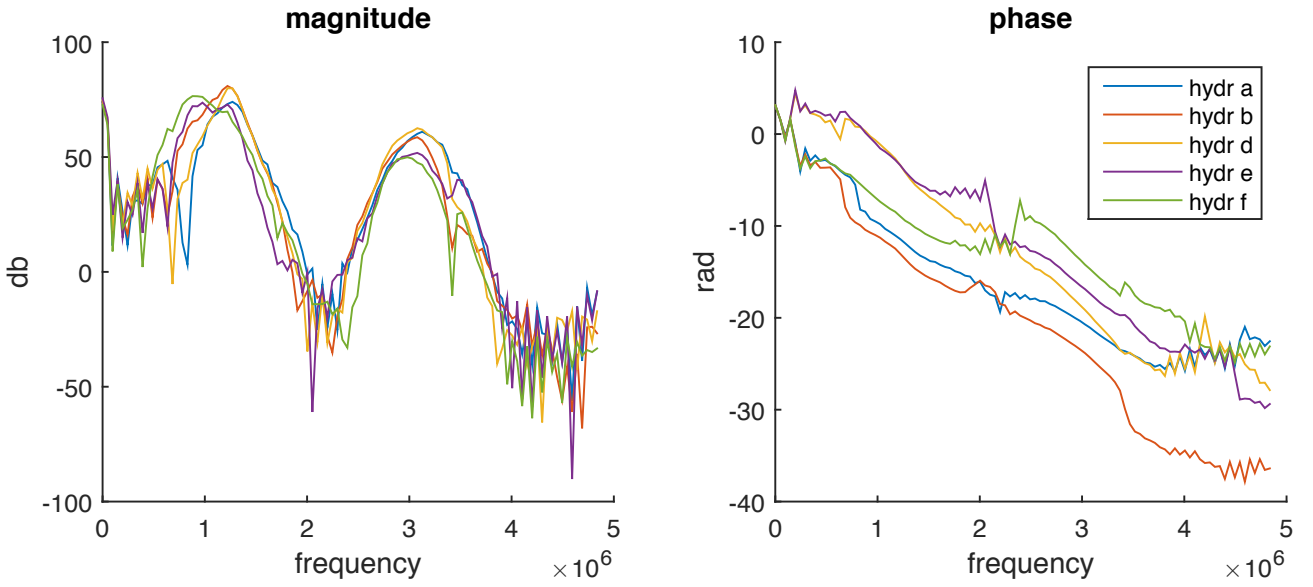


**Figure 42.:** Detail in analysis towards frequency domain of the first received pulses through a glass sample of repeated measurements. (Pulse in time domain is shown in fig. 40)

### 3.2.3. Sample's thickness resonances

The code provided by us biomat contains a program to estimate material properties from the measured first order thickness resonance in the ultrasonic transmission coefficient of a homogeneous plate at normal incidence. It obtains the following material properties: plate density, plate thickness, ultrasound velocity in the plate, ultrasound attenuation coefficient at resonant frequency in the plate and variation of the attenuation coefficient with the frequency assuming a power law. In order to do so, the amplitude spectrum and phase spectrum must be introduced into the code. More precisely a table containing a column for the frequency [Hz], one column that contains the amplitude spectrum of the measurement [dB] - the amplitude spectrum of the calibration (without sample) [dB] and a third column that contains the phase spectrum of the measurement [rad] - the phase spectrum of the calibration [rad]. Furthermore, an input specifying the experimental conditions can be provided if different from default (tab. 3).

**Table 3.:** Input to the program estimating material properties from thickness resonances of plates. Default data for a run on test data (membrane; air-coupled ultrasound) and adjusted input for under water measurement.

	default	water
Density of the fluid where the plate is located [kg/m <sup>3</sup> ]	1.2	1
Ultrasound velocity in this fluid [m/s]	343	1482.3
Loss in dB measured from the resonance peak to limit the analysis to this frequency band [dB]	10	20
Maximum number of steps allowed in the Gradient Descent	400	400
Step size in the Gradient Descent, constant	0.01	0.01
Minimum increment of the error allowed in the Gradient Descent, if no, the routine is interrupted and values returned	0.99999	0.99999
Option for graphical display 1: on, 0: off	1	1

A run with a set of test data provided with the code, obtained for a membrane with thickness 140 µm (micrometer) and density 340 kg/m<sup>3</sup> (size and weight), yields expected results (fig. 43 and tab. 4).

**Table 4.:** Output of the program estimating material properties from thickness resonances of plates. Results obtained for a run on test data (membran, air-coupled ultrasound) and results obtained for measurements (under water) of a glass sample. Also, reference values to compare are provided for the glass sample (density of glass [www.engineeringtoolbox.com](http://www.engineeringtoolbox.com), July 2016). IEE: Initial error estimation, FEE: Final error estimation.

	Test data	Measurement glass plate	Reference value
<b>Plate thickness [m]</b>	0.0001380709721	0.000990984622982	0.001
<b>Ultrasound velocity [m/s]</b>	367.268785786	5712.63669634	4540
<b>Attenuation coefficient [Np/m]</b>	454.488313512	100.139679771	
<b>Plate density [kg/m<sup>3</sup>]</b>	343.797114707	11.391844337	2400-2800
<b>Exponent in the attenuation vs freq power law</b>	1.9	1.9	
<b>Resonant frequency [Hz]</b>	1330000.0	2882303.4	2270000
<b>IEE Magnitude spectrum</b>	1.37190371749	8.72714309117	
<b>IEE Phase Spectrum</b>	3.50190587855	14.5866509219	
<b>FEE Magnitude spectrum</b>	0.239919382548	8.68468643416	
<b>FEE Phase spectrum</b>	0.678075637168	13.9501078535	
<b>Number of steps in the GD routine</b>	65	3	
<b>Loss from peak for bandwidth [dB]</b>	10.0	20.0	
<b>Q-factor of the resonance</b>	22.1666666667	29.5	
<b>Maximum of the Magnitude spectrum [dB]</b>	-18.7	-1.266453	
<b>Running time [s]</b>	4.07999992371	5.02999997139	
<b>Maximum number of steps allowed in GD routine</b>	400.0	400.0	
<b>Step size in GD routine</b>	0.01	0.01	
<b>Minimum error improvement for another step in GD</b>	0.99999	0.99999	

Processing the results of the actual measurements on the other hand did not provide satisfying results yet. To obtain the sample's thickness resonance and model its transmission coefficient, the measured magnitude and phase spectra have been processed by taking the difference of measured spectra with and without sample. For the pulses of the measurement shown in fig. 35, a detail in the range of 2 MHz of the so obtained spectrum is shown in fig. 44. Only a part of it has been taken to further analysis (thick blue line).

The output for this spectrum (fig. 45 and tab. 4) gives values not too bad for thickness and velocity but in a very different size range for density. In the graphical output dispersion in the measured values is apparent and the fitted transmission coefficient does not retrace the experimental data. Also the resonance frequency at 2.88 MHz does not match the expected resonance frequency at 2.27 MHz.

However, it is noticeable that in the vicinity of 2 MHz a local peak is visible. Also, if one compares the measured spectrum with and without sample (fig. 44), the main difference between them is a local minimum between 1.5 and 2 MHz and a peak around 2 MHz that appear in the spectrum with sample but not in the spectrum without sample. Noticeable is that a similar pattern can be found in some of the reproducibility measurements (fig. 42 green line), as well as in the measurements of different positions of the sample (fig. 38) and for different distances (appendix

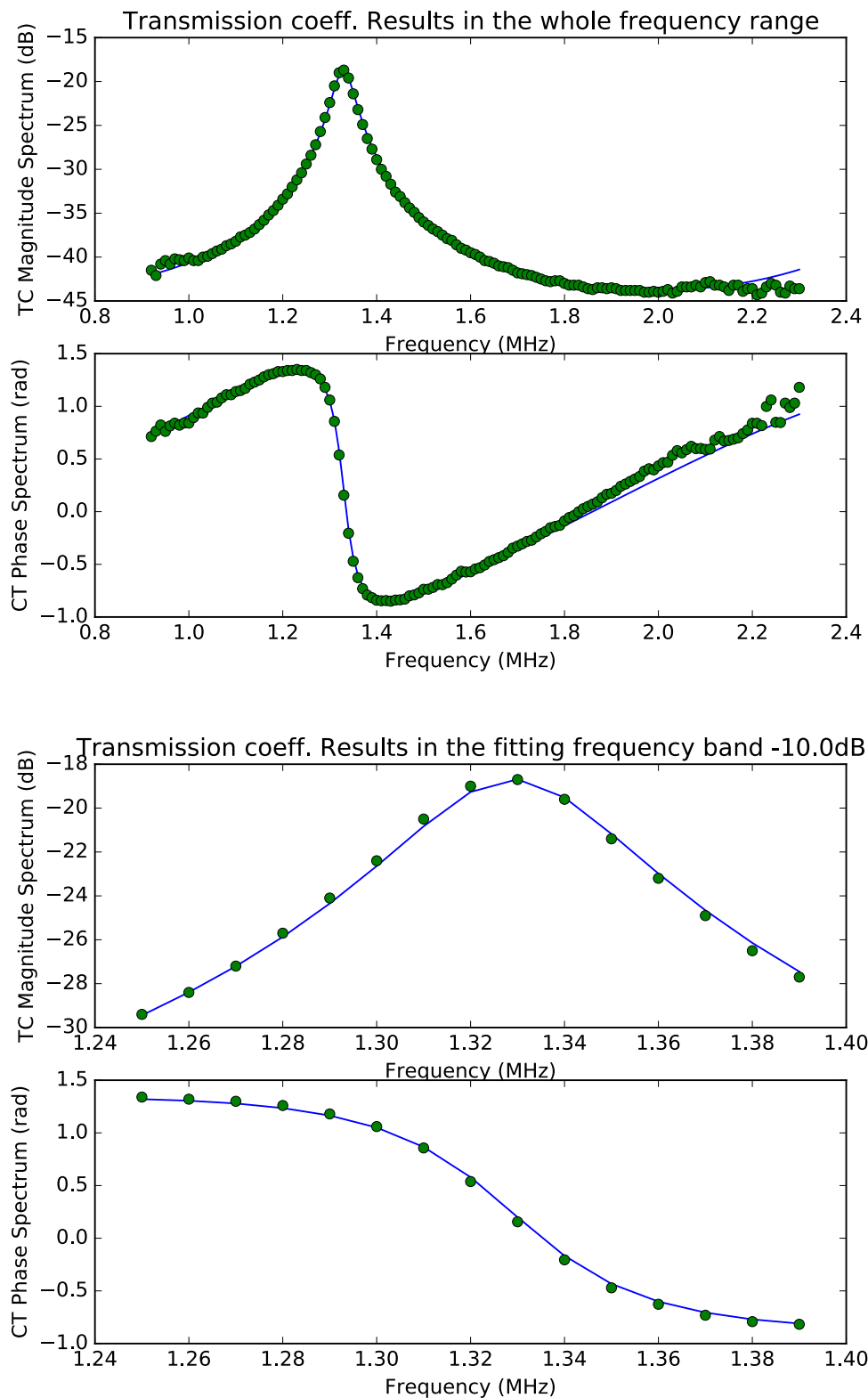


**Figure 43.:** Transmission coefficient spectra with fitted theoretical transmission coefficient of test data for a membran measured with air-coupled ultrasound.

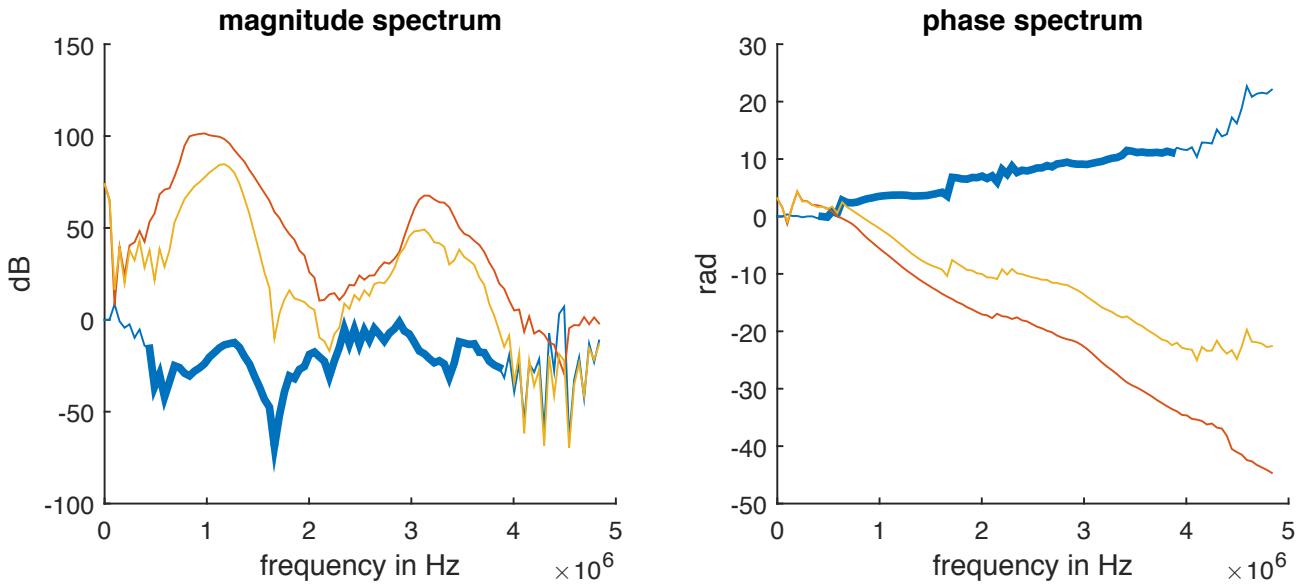


**Figure 44.:** Transmission coefficient spectrum (magnitude and phase) for a glass sample (blue line), obtained by taking the difference of measured pulse with sample (red line) and without sample (yellow line). Only the part marked by a thick blue line has been processed in further analysis.

B) but at frequencies between 3.5 and 4 MHz. A hint of this pattern between 3.5 and 4 MHz is also visible in the spectrum here (fig. 44).

As this pattern is only observed in measurements with sample in between and at frequencies roughly one doubling the other, it is obvious that this behavior could be related to the first and second thickness resonances of the sample. However, it remains unclear why the local minimum and peak are sometimes found at the first resonance, sometimes at the second and sometimes not at all. Probably the observation is very sensitive to the sample's orientation and alignment between transducer and hydrophone, two parameters that are slightly modified when setting up a new experiment run. On the other hand the fact that there are only local maxima excludes the interpretation of thickness resonances as they are per definition the maximum values in the transmission coefficient spectrum. The fitting procedure finds these maximum values (fig. 45). Somehow, even though there is a noticeable difference at frequencies around the expected first or second resonance between spectrum with and without sample, these differences are smaller than the overall discrepancy between the two spectra and thus gets lost. No clear thickness resonance can be seen and thus the model fitting does not yield values matching the expectations.

The other parameter not taken into account in the analysis so far is the phase spectrum.

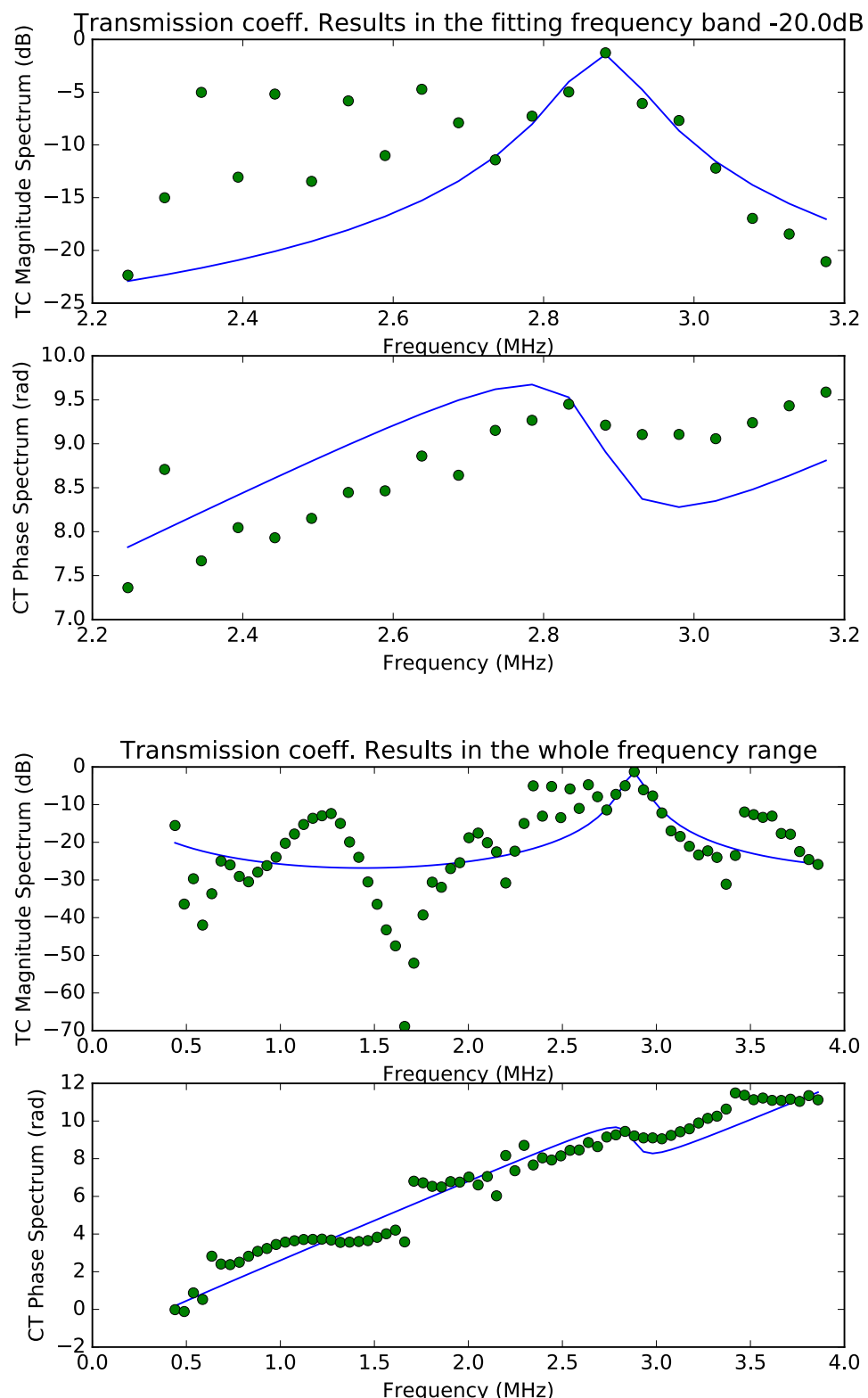


**Figure 45.:** Transmission coefficient spectra with fitted theoretical transmission coefficient of a measured glass sample.

## **4. Conclusion and way forward**

In the course of this project a setup for underwater through transmission ultrasonic measurements has been constructed and shown to work. Reproducible measurements have been carried out and the influence of distance between transducer and hydrophone as well as the position of a sample inbetween both have been investigated. However, some crucial parts of the setup need to be analysed further yet, such as the influence of the sample's orientation (angle) as well as the alignment of transducer and hydrophone, to gain a better understanding of the obtained signal.

The setup proved practical in measuring as well as changing sample. Nevertheless it could be easily improved by introducing a scaled bar next to the rods (holes are already provided) to enable distance measuring. Furthermore a better adjustment and also a measurement of angles is desireable.

Unfortunately the analysis of thickness resonances to obtain the sample's properties has not been successfull yet, even if a test run proved the program to work and to be installed correctly. Comparing the results of measurements with and without a glass sample in the ultrasonic pathway, a different pattern is apparent but not consistent. No clear thickness resonances could be observed. Therefore on the one hand the measurement settings of the pulser/receiver should be explored further and also the sent pulse should be analysed in order to gain a better understanding what exactly is happening in the measurement and which frequencies are covered by the sent pulse. On the other hand, the data analysis could be improved. In general, more attention should be paid to the phase spectrum which has not been taken into consideration in this work a lot.

Once the excitation and measurement of thickness resonances succeeds and material properties can be obtained by the program, other samples can be measured. Also, by getting in touch with the Ultrasounds for Biological Applications and Material Science Group, the code for running the two-layered model might be available and the data could be analysed towards this end as well.

Literature provides interesting results for plant leaves that could be elaborated further. Moreover also other (layered) biological structures such as insect wings, fruit shells, bones or seashells could be interesting samples for ultrasonic investigation.

# Bibliography

- Álvarez-Arenas, T. (2003a). Air-coupled ultrasonic spectroscopy for the study of membrane filters. *Journal of Membrane Science*, 213(1-2):195–207.
- Álvarez-Arenas, T. (2003b). A nondestructive integrity test for membrane filters based on air-coupled ultrasonic spectroscopy. *IEEE transactions on ultrasonics, ferroelectrics, and frequency control*, 50(6):676–685.
- Álvarez-Arenas, T. (2010). Simultaneous determination of the ultrasound velocity and the thickness of solid plates from the analysis of thickness resonances using air-coupled ultrasound. *Ultrasonics*, 50(2):104–109.
- Álvarez-Arenas, T., Sancho-Knapik, D., Peguero-Pina, J., and Gil-Pelegrín, E. (2009a). Determination of plant leaves water status using air-coupled ultrasounds. *IEEE International Ultrasonics Symposium Proceedings*, pages 771–774.
- Álvarez-Arenas, T., Sancho-Knapik, D., Peguero-Pina, J., and Gil-Pelegrín, E. (2009b). Non-contact and noninvasive study of plant leaves using air-coupled ultrasounds. *Applied physics letters*, 95:193702–1–193702–3.
- Collazos-Burbano, D., Cuello, J., Torres, G., Barandica, A., and Álvarez-Árenas, T. (2014). Air-coupled ultrasound spectroscopy and its potential application in agro-industry. *2014 XIX Symposium on Image, Signal Processing and Artificial Vision*, pages 1–5.
- Fariñas, M. and Álvarez-Arenas, T. (2014). Ultrasonic assessment of the elastic functional design of component tissues of phormium tenax leaves. *Journal of the Mechanical Behavior of Biomedical Materials*, 39:304–315.
- Fariñas, M. and Álvarez-Arenas, T. (2015). A layered acoustic model for the thickness resonances of plant leaves. *The 22<sup>nd</sup> International Congress on Sound and Vibration, Florence*, pages 1–8.
- Fariñas, M., Sancho-Knapik, D., Peguero-Pina, J., Gil-Pelegrín, E., and Álvarez Arenas, T. (2014). Monitoring plant response to environmental stimuli by ultrasonic sensing of the leaves. *Ultrasound in Medicine & Biology*, 40(9):2183 – 2194.
- Fukuhara, M. (2002). Acoustic characteristics of botanical leaves using ultrasonic transmission waves. *Plant Science*, 162(4):521–528.
- Fulgham, P. (2013). Physical principles of ultrasound. In Fulgham, P. and Gilbert, B., editors, *Practical Urological Ultrasound*, pages 9–26. Springer Science+Business Media, New York.
- Haines, N., Bell, J., and McIntyre, P. (1978). The application of broadband ultrasonic spectroscopy to the study of layered media. *The Journal of the Acoustical Society of America*, 64(6):1645–1651.
- Kadereit, J., Körner, C., Kost, B., and Sonnewald, U. (2014). *Strasburger - Lehrbuch der Pflanzenwissenschaften*, chapter 2.2 Dauergewebe; 3.3.1 Laubblatt. Springer Spektrum, Berlin Heidelberg.

- Leisure, R. G. and Willis, F. A. (1997). Resonant ultrasound spectroscopy. *Journal of Physics: Condensed Matter*, 9(28):6001–6029.
- Magnus, K., Popp, K., and Sextro, W. (2013). *Schwingungen. Physikalische Grundlagen und mathematische Behandlung von Schwingungen*, chapter *Grundbegriffe und Darstellungsmittel*, pages 1–17. Springer Fachmedien, Wiesbaden.
- Maulik, D. (2005). Physical principles of doppler ultrasonography. In Maulik, D., editor, *Doppler ultrasound in obstetrics and gynecology*, pages 9–17. Springer-Verlag, Berlin Heidelberg.
- Maynard, J. (1996). Resonant ultrasound spectroscopy. *Physics today*, 49(1):26–31.
- McClements, D. and Gunasekaran, S. (1997). Ultrasonic characterization of foods and drinks: Principles, methods and applications. *Critical Reviews in Food Science and Nutrition*, 37(1):1–46.
- NDT (online). NDT Resource Center. <https://www.nde-ed.org>. Accessed: May 2016.
- Novoa-Díaz, D., García-Álvarez, J., Chávez, J., Turó, A., García-Hernández, M., and Salazar, J. (2012). Comparison of methods for measuring ultrasonic velocity variations during ageing or fermentation of food materials. *IET Science, Measurement and Technology*, 6(4):205–212.
- Pain, H. (2005). *The physics of vibrations and waves*, chapter 5: Transverse Wave Motion, 6: Longitudinal Waves. John Wiley & Sons Ltd, Chichester.
- Parker, M. (2010). *Digital Signal Processing. Everything you need to know to get started*. Elsevier Inc., Burlington.
- Sachse, W. and Pao, Y. (1978). On the determination of phase and group velocities of dispersive waves in solids. *Journal of Applied Physics*, 49(8):4320–4327.
- Sancho-Knapik, D., Álvarez-Arenas, T., Peguero-Pina, J., Fernández, V., and Gil-Pelegrín, E. (2011). Relationship between ultrasonic properties and structural changes in the mesophyll during leaf dehydration. *Journal of Experimental Botany*, 62(10):3637–3645.
- Sancho-Knapik, D., Álvarez-Arenas, T., Peguero-Pina, J., and Gil-Pelegrín, E. (2010). Air-coupled broadband ultrasonic spectroscopy as a new non-invasive and non-contact method for the determination of leaf water status. *Journal of Experimental Botany*, 61(5):1385–1391.
- Sancho-Knapik, D., Calás, H., Peguero-Pina, J., Fernández, A., Gil-Pelegrín, E., and Álvarez-Arenas, T. (2012). Air-coupled ultrasonic resonant spectroscopy for the study of the relationship between plant leaves' elasticity and their water content. *IEEE Transactions on Ultrasonics, Ferroelectrics, and Frequency Control*, 59(2):319–325.
- Schrope, B. and Goel, N. (2014). Physical principles of ultrasound. In Hagopian, E. and Machi, J., editors, *Abdominal ultrasound for surgeons*, pages 7–15. Springer Science+Business Media, New York.
- Tempkin, S. (1981). *Elements of acoustics*, chapter 3.3 Transmission through a wall. John Wiley & Sons, Inc., New York.
- us biomat (online). Ultrasound for biological applications and materials science <https://us-biomat.com/>. Accessed: May 2016.
- Wang, M. and Pan, N. (2008). Predictions of effective physical properties of complex multiphase materials. *Materials Science and Engineering R Reports*, 63(4):1–30.

- Williams, D. (2012). The physics of ultrasound. *Anaesthesia and Intensive Care Medicine*, 13(6):264–268.
- WolframMathWorld (online). <http://mathworld.wolfram.com/InverseProblem.html>. Accessed: May 2016.

# **Appendix**

## A. Ultrasonic Spectroscopy “How to” guide

The setup allows ultrasonic through transmission measurements under water.

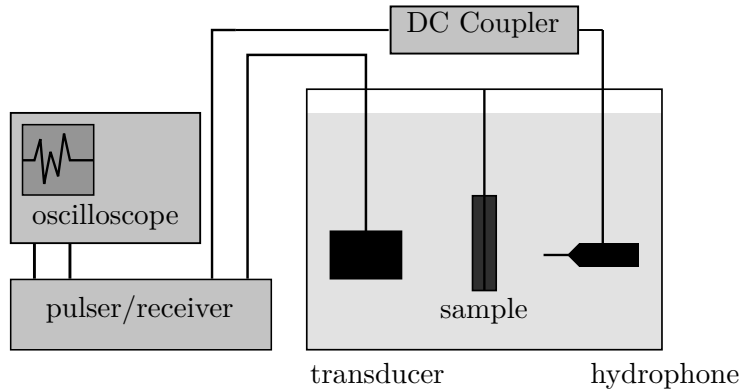


**Figure 46.:** Experimental Setup. Transducer and hydrophone are immersed in a fish tank filled with distilled water. The pulser/receiver drives the transducer to launch a signal through the sample to the hydrophone, from where it is then transferred back to the pulser/receiver again for amplification and filtering and finally the signal is displayed on the oscilloscope.

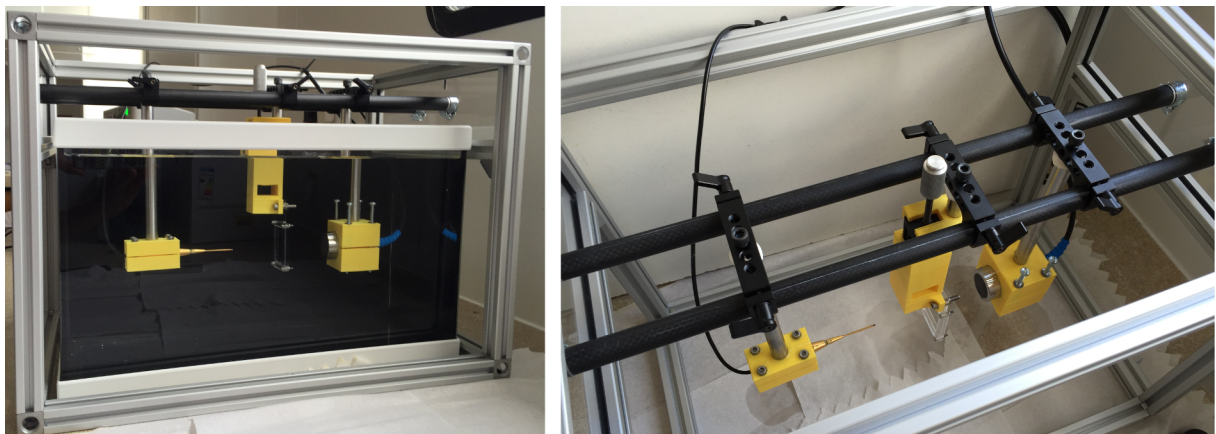


**Figure 47.:** Experimental Setup. The actual measurement situation is shown (*left*) as well as the scaffold removed from the fish tank (*right*). Slides to adjust distances as well as positioner for the adjustment of sample height are visible.

### Prior to first use

- Make sure you have enough space available to comfortably put measurement equipment, fish tank and scaffold next to each other and still have room for sample mounting.
- Fill up the fish tank with distilled water.
- Adjust the position of hydrophone and transducer holder. To do so, put only the upper part of the holder on and screw silver rod to slide. If it is completely screwed to the upper screw going through the slide, the holders should point straight and they should neither be too loose nor too tight so that a small adjustment of the angle is possible. If necessary, put some rubber material between silver rods and slides to stabilize the construction. If they do not point straight adjust by loosening the lower screw fixing holder to silver rod and screw on again in the correct angle.

- Take off holders and silver rods and carefully clamp preamplifier and transducer between upper and lower part of the holders and screw together. Take care to screw evenly. Re-mount silver rods to slides.
- Connect from the pulser/receiver “T/R” to transducer, ”Through” to DC Coupler and DC coupler to preamplifier, “Receiver output” to oscilloscope and “Trig/Sync” to “Trig in” on the oscilloscope. Set pulser/receiver to through transmission mode and internal trigger on the front panel.
- Very carefully mount hydrophone needle\* on preamplifier. The sensor on the needle tip is very sensible and must not be touched.

## **Measurements**

- If necessary prepare sample and fix into frame. Frame sizes 4x4 cm, 3x3 cm and 2x2 cm are available, if other sizes are needed they can be easily produced from acrylic plastic (3 mm thick) with the overall sizes given in the figure below.
- Carefully mount frame on sample holder and position as needed.
- Remove transducer and hydrophone protective covers.
- Make sure transducer and hydrophone slides are in a position not too extreme to fit easily into fish tank and no cables are dangling loose along the scaffold.
- Move scaffold over fish tank and adjust distances/angles as needed.
- Turn pulser/receiver and DC Coupler on and adjust parameters. See pulser/receiver manual for the different options and what the relative 16-step increments on e.g. the amplitude button mean in absolute values.
- The following settings could be used for a start: Pulse repetition frequency (PRF) 1 (100 Hz), pulse amplitude 7 (164.0625 V), pulse energy 1 with Z high, damping 1 ( $331\ \Omega$ ), relative gain 38, HP Filter out and LP Filter at 35 MHz.
- Move hydrophone slide slightly to and fro to identify the received signals as opposed to the sent pulse.
- Adjust oscilloscope to desired resolution.
- Take measurement(s) and save to USB.
- Turn pulser/receiver and DC Coupler off, remove scaffold.
- Carefully remove sample frame, remove sample and mount frame back on the holder and repeat measurements if necessary.
- For storage carefully remove hydrophone needle\* and put protective cover back on needle and transducer.

\*At the point when this report was written, the removal of the hydrophone needle turned out to be problematic as it stuck on the preamplifier. Hoping that this problem will be solved by the time when this report is used to continue the measurements, an easy removal of tip is implied in the description.

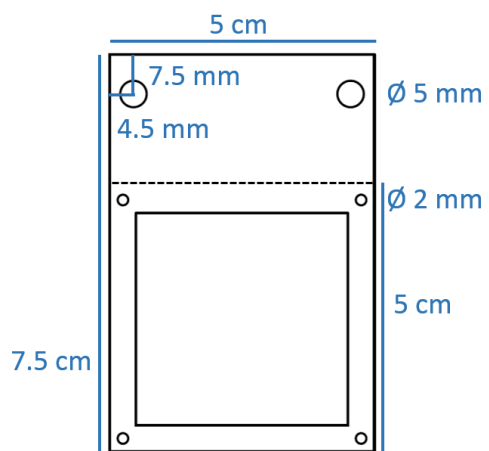


**Figure 48.:** Size of sample frame. Resize inner frame as desired.

## EPS RISK ASSESSMENT FORM

Reference Number  

### SCHOOL OF ENGINEERING AND PHYSICAL SCIENCES HERIOT-WATT UNIVERSITY

<b>Location/s of Activity</b> Building (JC, NS, DB, WP, EM) and Room Number	EM      3.14
--	--------------

<b>Category of Activity</b> e.g. Laboratory Class, UG Project, MSc Project, Research Project, Office Work, Workshop	Research Project (Internship)
---	-------------------------------

<b>Title of Activity</b>	Ultrasound Spectroscopy (underwater)
--------------------------	--------------------------------------

<b>Nature of Activity</b> Include any relevant literature references. More-detailed schemes of work may be appended	<p>Ultrasonic measurements in through-transmission set up under water</p>
--	---

<b>Those Affected</b> Printed Names	Signatures	Dates	Status*
Frederike Klimm		5.7.16	visiting scholar/intern

\*State whether Academic Staff (A), Academic Related Staff (AR), Technical Staff (T), Office Staff (O)  
RA, PhD, MPhil, MSc, Undergraduate (UG), Visitor (V), Other – specify  
Cleaning Staff (CS), Estates (E), Contractor (C) – an authorised Permit to Work form must be attached

<b>Name and Status of Assessor</b> Printed Name	Signature	Date	Status
Anne Bernassau		4/07/16	Ass. Prof

<b>Name and Status of Supervisor (for Students and Researchers) or Line Manager (for Permanent Staff other than Academics)</b> Printed Name			
Nave De Sainville	Signature	Date	Status
		8/7/16	Prof

## EPS RISK ASSESSMENT FORM

### HAZARDS & SPECIFIC CONTROL MEASURES

Identify each applicable hazard; examples are given below, cross as appropriate

Decide the residual risk to workers with the control measures described on Pages 2-3 of this form in place

Potential Hazard	Additional Action		
Chemicals	<input type="checkbox"/> Oils/Lubricating Materials	<input type="checkbox"/> Complete a Coshh RA Form and attach it to this Form	
Solvents	<input type="checkbox"/> Gases or Liquid Gases	<input type="checkbox"/> Or for Perkin Building only: complete Page-4 of this Form	
Biological Substances	<input type="checkbox"/> Powders or Dust		
Glues/Adhesives	<input type="checkbox"/> Fume emissions		
Radio-active Sources	<input type="checkbox"/> X-rays	<input type="checkbox"/> Contact Building Radiation Protection Supervisor	
UV	<input type="checkbox"/> Microwave or RF Sources		
Visible or Non-Visible Lasers		<input type="checkbox"/> Contact Building Laser Safety Officer	
Asbestos		<input type="checkbox"/> Contact Building Superintendent and University Health, Safety & Risk Office	
All Electrical Equipment		<input checked="" type="checkbox"/> Ensure Equipment is within its test period	

### Further Examples

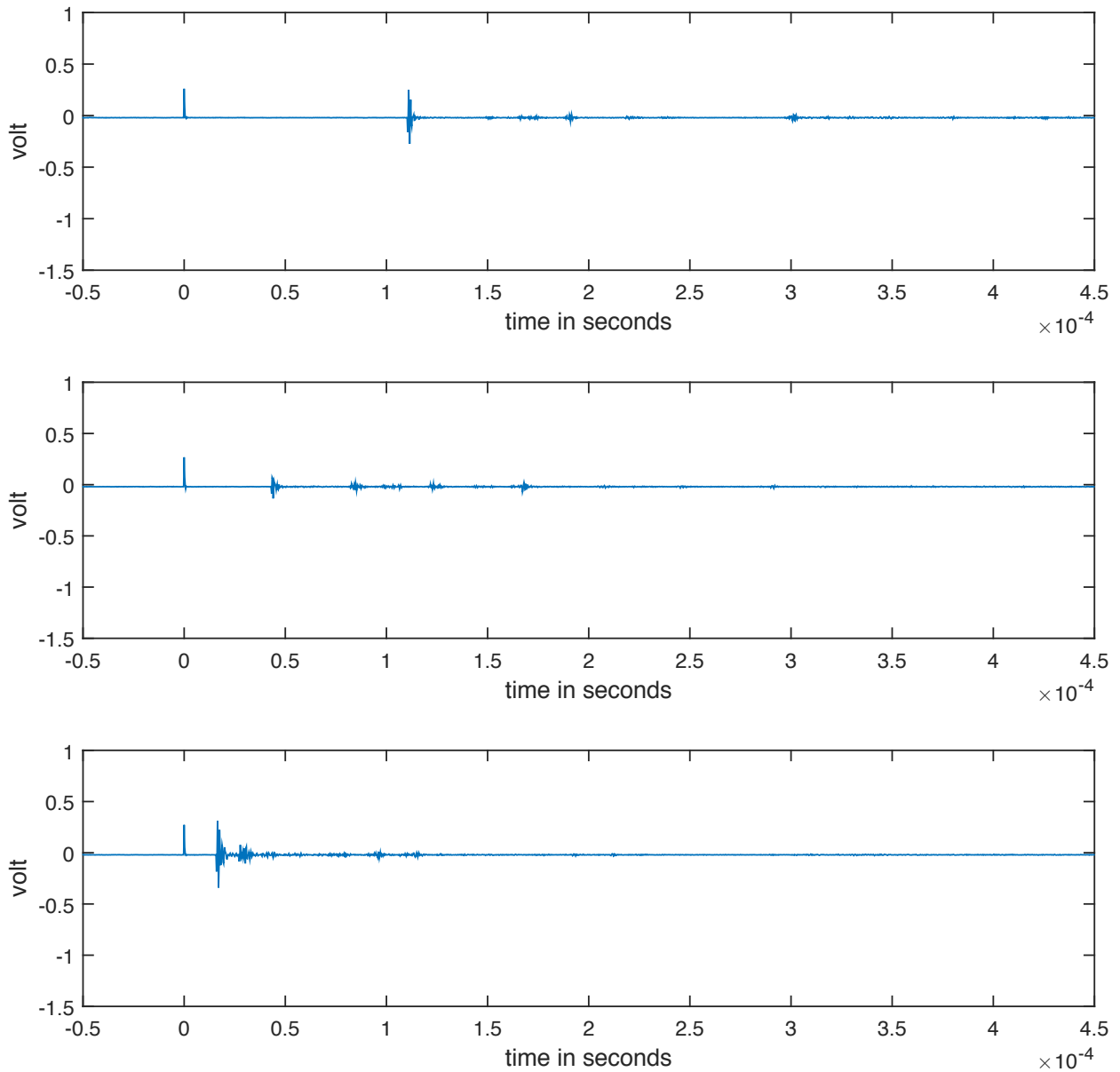
AC or DC Supplies over 50 Volts	<input checked="" type="checkbox"/>	Use of Display Screen Equipment (2 hours per day or more most days)	<input type="checkbox"/>
Servicing Electrical Equip. or Supplies	<input type="checkbox"/>		
Hot surfaces or Ovens	<input type="checkbox"/>	Gas under Pressure	<input type="checkbox"/>
Flammability, Fires	<input type="checkbox"/>	Pressure/Vacuum Systems	<input type="checkbox"/>
Welding	<input type="checkbox"/>	Cryogens	<input type="checkbox"/>
Motors & Rotating Machines	<input type="checkbox"/>	Manual Handling	<input type="checkbox"/>
Power Drilling	<input type="checkbox"/>	Use of Slings or Shackles	<input type="checkbox"/>
Lathe Work or Milling	<input type="checkbox"/>	Use of Lifting Equipment or Jacks	<input type="checkbox"/>
Sharp Edges or Implements	<input type="checkbox"/>	Working at Height	<input type="checkbox"/>
Use of Vehicles	<input type="checkbox"/>	Water tanks	<input checked="" type="checkbox"/>
Working off campus	<input type="checkbox"/>	Diving	<input type="checkbox"/>
Noise	<input type="checkbox"/>	Others – Specify below	<input type="checkbox"/>

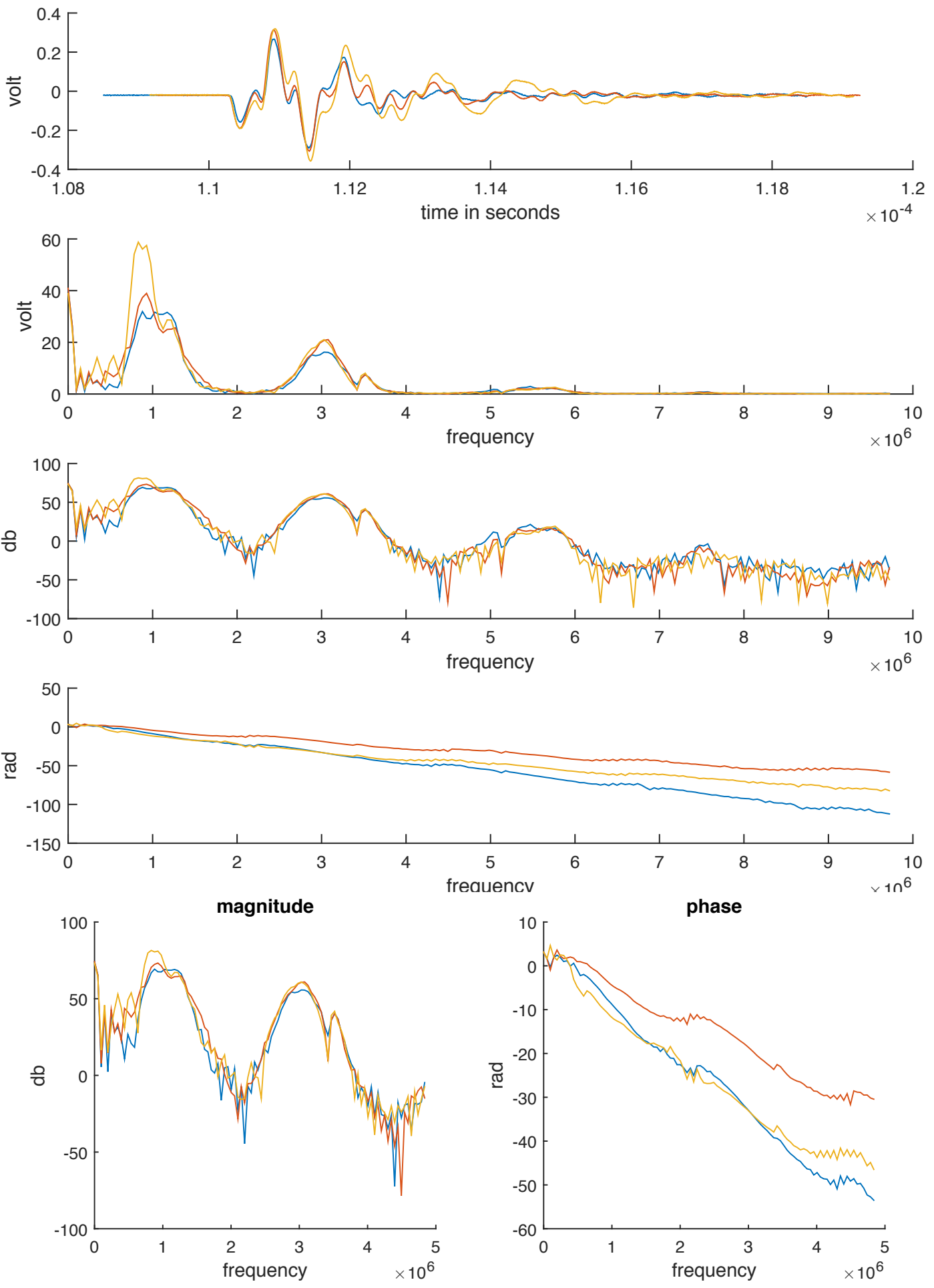
Identified Hazard	Specific Control Measures e.g. (24h) Fume Cupboard, Blast Screen, Safety Interlock, Personal Protection Equipment or Clothing (goggles, face-mask, safety foot-ware, etc) Tick if written procedures are available	Residual Risk Low, Med, High
DC coupler, pulses/receivers, oscilloscope mains operated	placed away from fish tank, special caution when moving scaffold, disconnect if gets in touch with water	Low
Shock + fire hazard whilst replacing fuses pulses/receivers (if necessary at all.)	ob's connect before replacing + only replace with fuses of same type + rating. See manual.	Low
electrical power cables in water; touching of water or metal components during operation (necessary)	• make sure cables are in order before starting • turn power off before moving	Low
→ Shock hazard in case of damaged cables	Scaffold into tank, turn power on without touching equipment (in case of damage electrical short might appear)	Low

## B. Distance shift

Results for measurements at different distances of transducer to receiver with a glass sample in between. Covering the entire signal (*top* distant, *middle* intermediate and *bottom* near) as well as the first received signal in detail (blue line distant, red line intermediate and yellow line near).

Distance shift - with sample

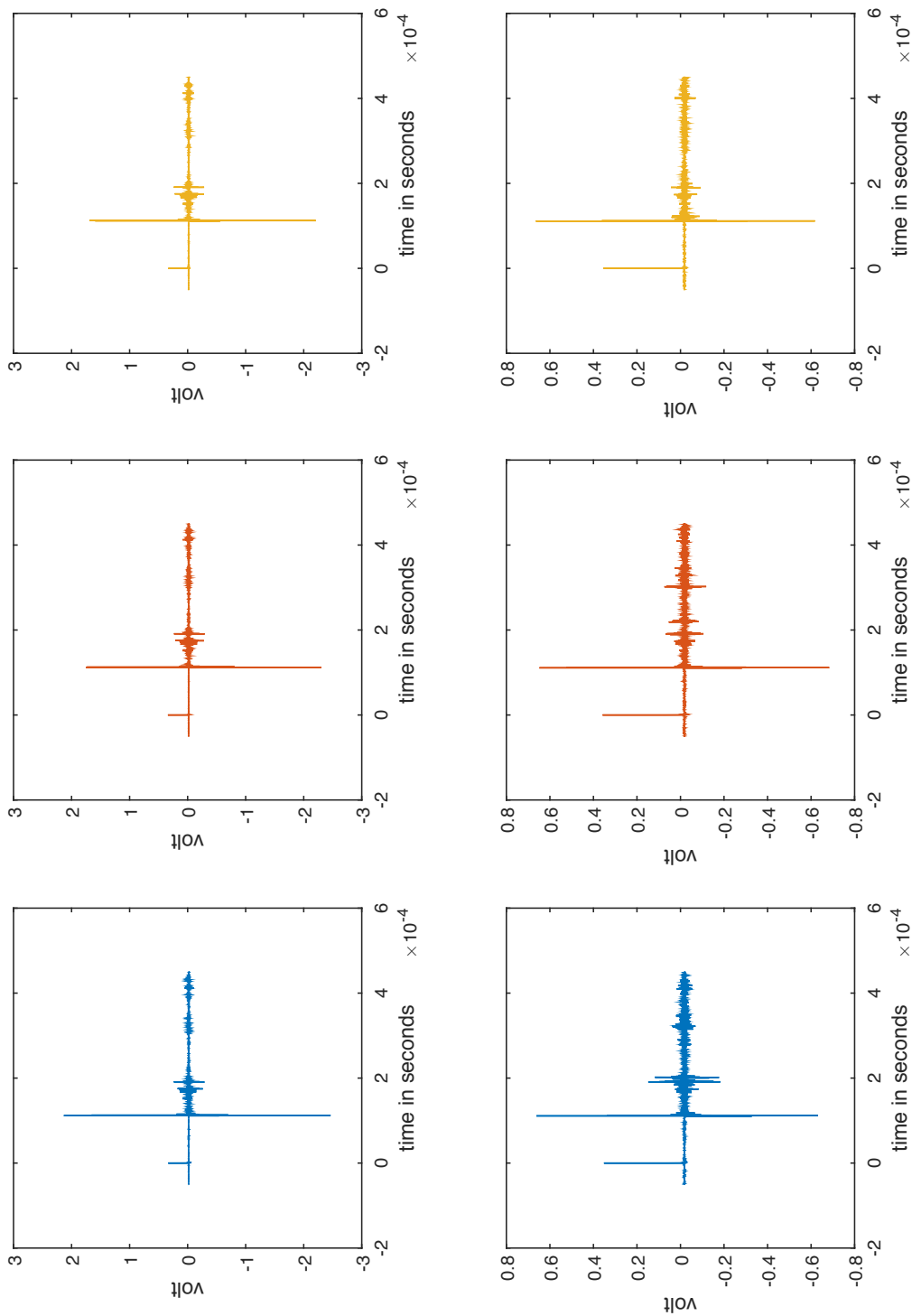




### C. Position shift

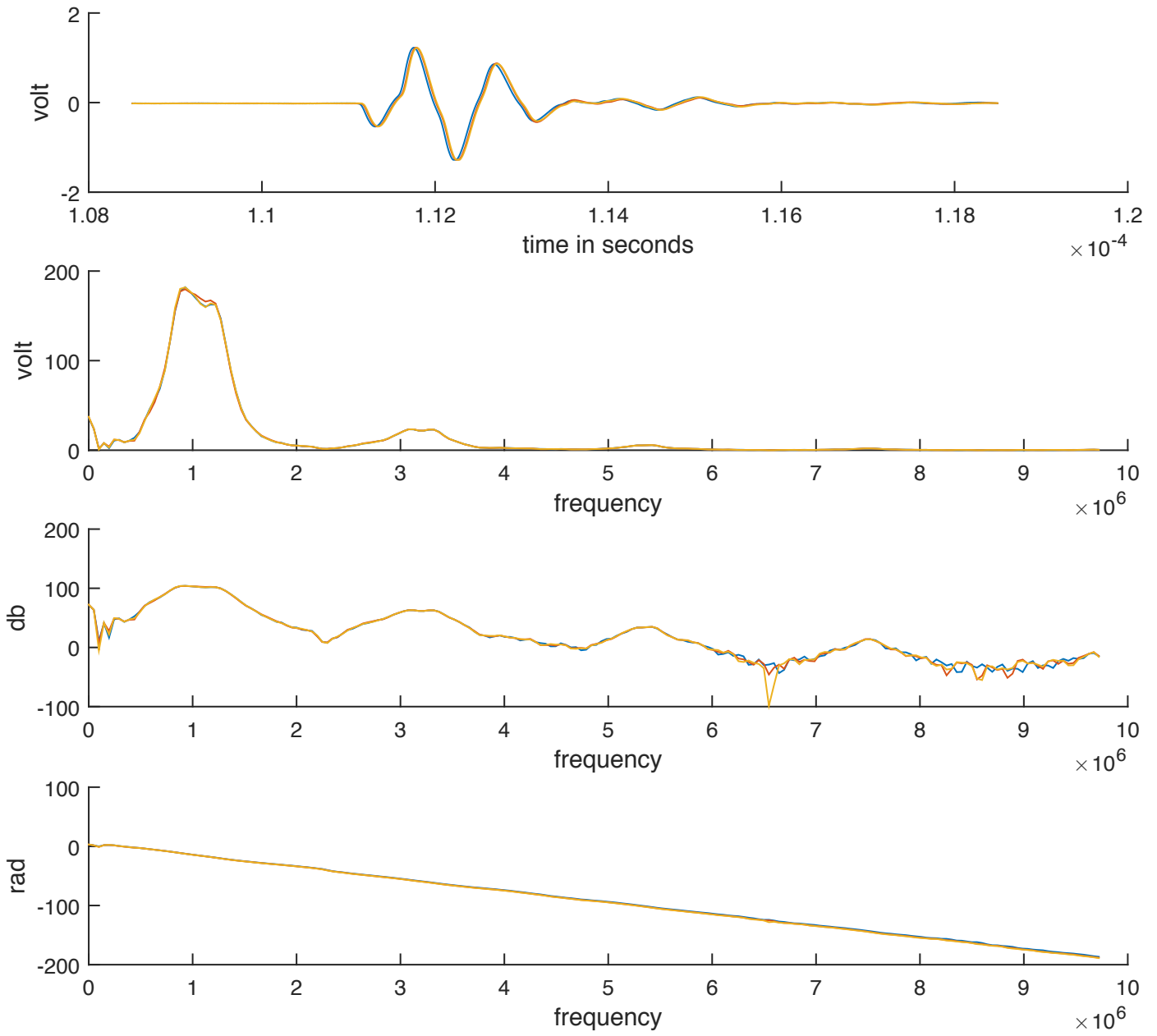
Measured signal from transducer to hydrophone with different positions of the sample holder in between (blue line near to hydrophone, red line middle and yellow line near transducer). Measurements shown above are taken with the sample (glass slide) mounted on holder, measurements below without.

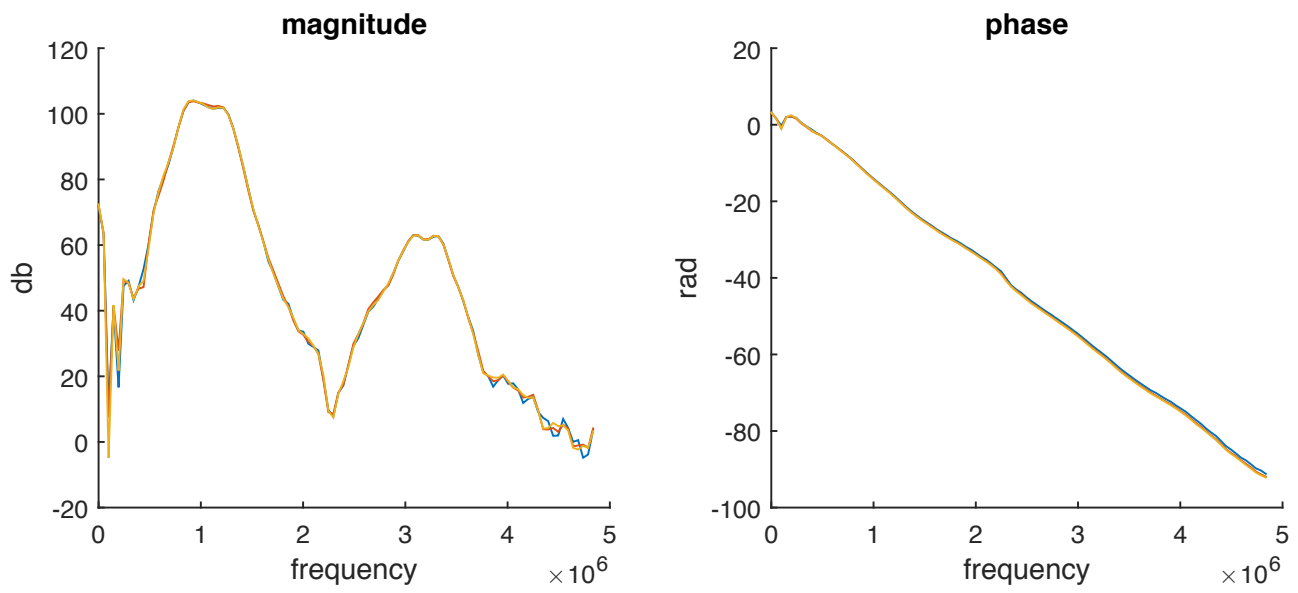
Position shift - without and with sample



First received pulse without the sample in between transducer and hydrophone. Comparison of the sample positioned near the hydrophone (blue line), in the middle (red line) and near the transducer (yellow line) in the time domain (*top*), the magnitude spectrum (*middle two*) and the phase spectrum (*bottom*), as well as detail in magnitude and phase spectrum.

### Position shift - without sample





## D. Reproducibility

Analysis in frequency domain of the first received pulse of repeated measurements (hydr a, b, d-f) without a sample in between transducer and hydrophone, as well as detail in magnitude and phase spectrum.

hydrophone tests - without sample

